

# Several Solution Techniques

In this chapter, we turn our attention primarily to an introduction to numerical methods, but also consider the analytical technique of *separation of variables* for the solution of Laplace's equation in two dimensions and a geometrical method based on *field mapping* for the determination of transmission line parameters.

For the numerical techniques, we are interested in the application of well-known methods for solving integral equations and partial differential equations to the numerical solution of Maxwell's equations and equations involving potential. In this context, we shall consider four methods: (1) the finite-difference method, leading to the solution of Laplace's equation in two dimensions by using appropriate finite-difference approximations to the derivative terms; (2) the method of moments, involving the inversion of an integral equation relating the electric potential to charge distribution by approximating the integral as a summation; (3) the finite-element method, also for solving Laplace's equation in two dimensions, but based on the minimization of electric energy expressed as an integral over the region of interest; and (4) the finite-difference time-domain method, for solving the one-dimensional wave equation or the first-order differential equations leading to it by extending the finite-difference approximations to the time derivative terms. We shall also present several examples of applications, including the determination of transmission-line parameters and the time-domain analysis of an initially charged transmission line.

## 11.1 ANALYTICAL SOLUTION OF LAPLACE'S EQUATION

Considering Laplace's equation (5.61) and its expansion in Cartesian coordinates, given by (5.62), and assuming the potential to be independent of  $z$ , we obtain the two-dimensional Laplace's equation in  $x$  and  $y$  to be

$$\frac{\partial^2 V}{\partial x^2} + \frac{\partial^2 V}{\partial y^2} = 0 \quad (11.1)$$

Equation (11.1) is a partial differential equation in two dimensions. As we already discussed in Sec. 9.1, the technique by means of which it is solved is the “separation of variables” technique. It consists of assuming that the solution for the potential is the product of two functions, one of which is a function of  $x$  only and the second is a function of  $y$  only. Denoting these functions to be  $X$  and  $Y$ , respectively, we have

*“Separation  
of variables”  
technique*

$$V(x, y) = X(x)Y(y) \quad (11.2)$$

Substituting this assumed solution into the differential equation, we obtain

$$Y \frac{d^2 X}{dx^2} + X \frac{d^2 Y}{dy^2} = 0$$

Dividing both sides by  $XY$  and rearranging, we get

$$\frac{1}{X} \frac{d^2 X}{dx^2} = -\frac{1}{Y} \frac{d^2 Y}{dy^2} \quad (11.3)$$

The left side of (11.3) is a function of  $x$  only; the right side is a function of  $y$  only. Thus (11.3) states that a function of  $x$  only is equal to a function of  $y$  only. A function of  $x$  only other than a constant cannot be equal to a function of  $y$  only other than the same constant for all values of  $x$  and  $y$ . For example,  $2x$  is equal to  $4y$  for only those pairs of values of  $x$  and  $y$  for which  $x = 2y$ . Since we are seeking a solution that is good for all pairs of  $x$  and  $y$ , the only solution that satisfies (11.3) is that for which each side of (11.3) is equal to a constant. Denoting this constant to be  $\alpha^2$ , we have

$$\frac{d^2 X}{dx^2} = \alpha^2 X \quad (11.4a)$$

and

$$\frac{d^2 Y}{dy^2} = -\alpha^2 Y \quad (11.4b)$$

Thus, we have obtained two ordinary differential equations involving separately the variables  $x$  and  $y$ , starting with the partial differential equation involving both of the variables  $x$  and  $y$ . It is for this reason that the method is known as the separation of variables technique.

The solutions for (11.4a) and (11.4b) are given by

$$X(x) = \begin{cases} Ae^{\alpha x} + Be^{-\alpha x} & \text{for } \alpha \neq 0 \\ A_0 x + B_0 & \text{for } \alpha = 0 \end{cases} \quad (11.5a)$$

where  $A, B, A_0,$  and  $B_0$  are arbitrary constants, and

$$Y(y) = \begin{cases} C \cos \alpha y + D \sin \alpha y & \text{for } \alpha \neq 0 \\ C_0 y + D_0 & \text{for } \alpha = 0 \end{cases} \quad (11.5b)$$

where  $C, D, C_0,$  and  $D_0$  are arbitrary constants. Substituting (11.5a) and (11.5b) into (11.2), we obtain

$$V(x, y) = \begin{cases} (Ae^{\alpha x} + Be^{-\alpha x})(C \cos \alpha y + D \sin \alpha y) & \text{for } \alpha \neq 0 \\ (A_0 x + B_0)(C_0 y + D_0) & \text{for } \alpha = 0 \end{cases} \quad (11.6)$$

Equation (11.6) is the general solution for Laplace's equation in the two dimensions  $x$  and  $y$ . The arbitrary constants are evaluated from the boundary conditions specified for a given problem. We shall now consider two examples.

---

### Example 11.1 Application of analytical solution of Laplace's equation in two dimensions

Let us consider an infinitely long rectangular slot cut in a semi-infinite plane conducting slab held at zero potential, as shown by the cross-sectional view, transverse to the slot, in Fig. 11.1. With reference to the coordinate system shown in the figure, assume that a potential distribution  $V = V_0 \sin(\pi y/b)$ , where  $V_0$  is a constant, is created at the mouth  $x = a$  of the slot by the application of a potential to an appropriately shaped conductor away from the mouth of the slot not shown in the figure. We wish to find the potential distribution in the slot.

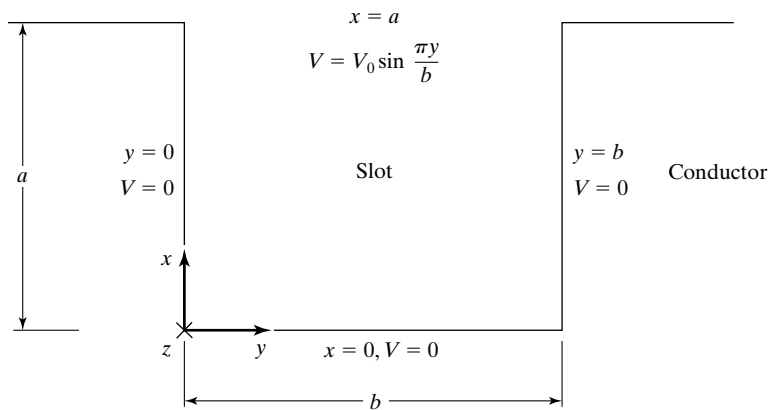


FIGURE 11.1

Cross-sectional view of a rectangular slot cut in a semi-infinite plane conducting slab at zero potential. The potential at the mouth of the slot is  $V_0 \sin(\pi y/b)$  volts.

Since the slot is infinitely long in the  $z$  direction with uniform cross section, the problem is two dimensional in  $x$  and  $y$  and the general solution for  $V$  given by (11.6) is applicable. The boundary conditions are

$$V = 0 \quad \text{for } y = 0, 0 < x < a \quad (11.7a)$$

$$V = 0 \quad \text{for } y = b, 0 < x < a \quad (11.7b)$$

$$V = 0 \quad \text{for } x = 0, 0 < y < b \quad (11.7c)$$

$$V = V_0 \sin \frac{\pi y}{b} \quad \text{for } x = a, 0 < y < b \quad (11.7d)$$

The solution corresponding to  $\alpha = 0$  does not fit the boundary conditions, since  $V$  is required to be zero for two values of  $y$  and in the range  $0 < x < a$ . Hence we can ignore that solution and consider only the solution for  $\alpha \neq 0$ .

Applying the boundary condition (11.7a), we have

$$0 = (Ae^{\alpha x} + Be^{-\alpha x})(C) \quad \text{for } 0 < x < a$$

The only way of satisfying this equation for a range of values of  $x$  is by setting  $C = 0$ . Next, applying the boundary condition (11.7c), we have

$$0 = (A + B)D \sin \alpha y \quad \text{for } 0 < y < b$$

This requires that  $(A + B)D = 0$ , which can be satisfied by either  $A + B = 0$  or  $D = 0$ . We, however, rule out  $D = 0$  since it results in a trivial solution of zero for the potential. Hence we set

$$A + B = 0 \quad \text{or} \quad B = -A$$

Thus the solution for  $V$  reduces to

$$\begin{aligned} V(x, y) &= (Ae^{\alpha x} - Ae^{-\alpha x})D \sin \alpha y \\ &= A' \sinh \alpha x \sin \alpha y \end{aligned} \quad (11.8)$$

where  $A' = 2AD$ .

Next, applying boundary condition (11.7b) to (11.8), we obtain

$$0 = A' \sinh \alpha x \sin \alpha b \quad \text{for } 0 < x < a$$

To satisfy this equation without obtaining a trivial solution of zero for the potential, we set

$$\sin \alpha b = 0$$

or

$$\alpha b = n\pi \quad n = 1, 2, 3, \dots$$

$$\alpha = \frac{n\pi}{b} \quad n = 1, 2, 3, \dots$$

Since several values of  $\alpha$  satisfy the boundary condition, several solutions are possible for the potential. To take this into account, we write the solution as the superposition of all these solutions multiplied by different arbitrary constants. In this manner, we obtain

$$V(x, y) = \sum_{n=1,2,3,\dots}^{\infty} A'_n \sinh \frac{n\pi x}{b} \sin \frac{n\pi y}{b} \quad \text{for } 0 < y < b \quad (11.9)$$

Finally, applying the boundary condition (11.7d) to (11.9), we get

$$V_0 \sin \frac{\pi y}{b} = \sum_{n=1,2,3,\dots}^{\infty} A'_n \sinh \frac{n\pi a}{b} \sin \frac{n\pi y}{b} \quad \text{for } 0 < y < b \quad (11.10)$$

On the right side of (11.10) we have an infinite series of sine terms in  $y$ , but on the left side we have only one sine term in  $y$ . Equating the coefficients of the sine terms having the same arguments, we obtain

$$A'_n \sinh \frac{n\pi a}{b} = \begin{cases} V_0 & \text{for } n = 1 \\ 0 & \text{for } n \neq 1 \end{cases}$$

or

$$\begin{aligned} A'_1 &= \frac{V_0}{\sinh(\pi a/b)} \\ A'_n &= 0 \quad \text{for } n \neq 1 \end{aligned}$$

Substituting this result in (11.9), we obtain the required solution for  $V$  as

$$V(x, y) = V_0 \frac{\sinh(\pi x/b)}{\sinh(\pi a/b)} \sin \frac{\pi y}{b} \quad (11.11)$$

We may now compute the potential at any point inside the slot, given the values of  $a$ ,  $b$ , and  $V_0$ . For example, for  $a = b$ , that is, for a square slot, (11.11) gives the potential at the center of the slot to be  $0.1993V_0$ .

### Example 11.2 Application of analytical solution of Laplace's equation in two dimensions

Let us assume that the rectangular slot of Fig. 11.1 is covered at the mouth  $x = a$  by a conducting plate that is kept at a potential  $V = V_0$ , making sure that the edges touching the corners of the slot are insulated, as shown in Fig. 11.2(a), and find the solution for the potential in the slot for this new boundary condition.

Since the boundary conditions (11.7a)–(11.7c) remain the same, all we need to do to find the required solution for the potential is to substitute the new boundary condition

$$V = V_0 \quad \text{for } x = a, 0 < y < b$$

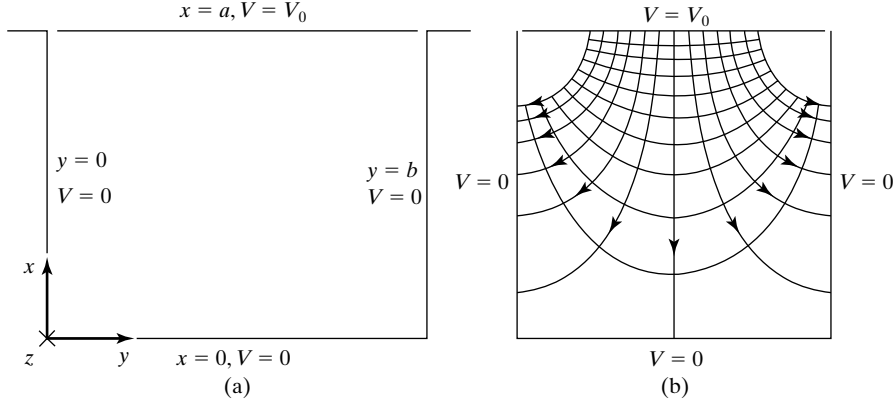


FIGURE 11.2

(a) Cross-sectional view of a rectangular slot in a semi-infinite plane conducting slab at zero potential and covered at the mouth by a conducting plate kept at a potential  $V_0$ .

(b) Equipotentials and direction lines of electric field in the slot for the case  $b/a = 1$

in (11.9) and evaluate the coefficients  $A'_n$ . Thus we have

$$V_0 = \sum_{n=1,2,3,\dots}^{\infty} A'_n \sinh \frac{n\pi a}{b} \sin \frac{n\pi y}{b} \quad \text{for } 0 < y < b \quad (11.12)$$

In this equation we have an infinite series on the right side, but the left side is a constant. Thus we cannot hope to obtain  $A'_n$  by simply comparing the coefficients of the sine terms having like arguments as in Example 11.1. If we do so, we get the result of  $V_0 = 0$  and all  $A'_n = 0$  since there is no constant term on the right side and there are no sine terms on the left side.

The way out of the dilemma is to make use of the so-called orthogonality property of sine functions, given by

$$\int_{y=0}^p \sin \frac{n\pi y}{p} \sin \frac{m\pi y}{p} dy = \begin{cases} 0 & n \neq m \\ \frac{p}{2} & n = m \end{cases}$$

where  $m$  and  $n$  are integers. Multiplying both sides of (11.12) by  $\sin \frac{m\pi y}{b} dy$  and integrating between the limits 0 and  $b$ , we have

$$\int_{y=0}^b V_0 \sin \frac{m\pi y}{b} dy = \int_{y=0}^b \sum_{n=1,2,3,\dots}^{\infty} A'_n \sinh \frac{n\pi a}{b} \sin \frac{n\pi y}{b} \sin \frac{m\pi y}{b} dy$$

The integration and summation on the right side can be interchanged, giving us

$$\int_{y=0}^b V_0 \sin \frac{m\pi y}{b} dy = \sum_{n=1,2,3,\dots}^{\infty} A'_n \sinh \frac{n\pi a}{b} \int_{y=0}^b \sin \frac{n\pi y}{b} \sin \frac{m\pi y}{b} dy$$

or

$$\frac{V_0 b}{m\pi} (1 - \cos m\pi) = \left( A'_m \sinh \frac{m\pi a}{b} \right) \frac{b}{2}$$

$$A'_m = \begin{cases} \frac{4V_0}{m\pi} \frac{1}{\sinh(m\pi a/b)} & \text{for } m \text{ odd} \\ 0 & \text{for } m \text{ even} \end{cases}$$

Substituting this result in (11.9), we obtain the required solution for the potential inside the slot as

$$V = \sum_{n=1,3,5,\dots}^{\infty} \frac{4V_0}{n\pi} \frac{\sinh(n\pi x/b)}{\sinh(n\pi a/b)} \sin \frac{n\pi y}{b} \quad (11.13)$$

The numerical values of potentials may now be computed for points inside the slot for given values of  $a$ ,  $b$ , and  $V_0$ , and equipotentials may be sketched by joining points having approximately the same potential values. The electric field lines can then be drawn orthogonal to the equipotentials. The resulting sketches for a square slot are shown in Fig. 11.2(b).

**K11.1.** Laplace's equation in two dimensions; Separation of variables technique.

**D11.1.** A conductor occupying the surfaces  $x > 0$ ,  $y = 0$  and  $y > 0$ ,  $x = 0$  is kept at zero potential. A second conductor occupying the surfaces  $xy = 2$ ,  $x > 0$ ,  $y > 0$ , is kept at a potential of 100 V. The edges where the conductors touch are insulated. The medium between the conductors is free space. Find the following in a  $z = \text{constant}$  plane: **(a)** the potential at  $x = 1$ ,  $y = 1$ ; **(b)** the electric field intensity at  $x = 1$ ,  $y = 2$ ; and **(c)** the surface charge density at  $x = 1$ ,  $y = 0$ .

*Ans.* **(a)** 50 V; **(b)**  $-(100\mathbf{a}_x + 50\mathbf{a}_y)$  V/m; **(c)**  $-50\epsilon_0$  C/m<sup>2</sup>.

## 11.2 NUMERICAL SOLUTION BY FINITE-DIFFERENCE METHOD

The finite-difference method is employed for solving differential equations, and it is perhaps the simplest method for that purpose. It consists of replacing the derivative terms in the differential equation by their finite-difference approximations and solving the resulting algebraic equations. To do this, the region of interest is discretized by selecting a set of grid points, and the derivatives of the function of interest at each grid point are expressed in terms of the values of the function at a subset of the grid points by using approximations such as the central-difference formulas. The resulting set of algebraic equations are solved for the values of the function at the grid points. We shall illustrate this first in one-dimension.

Thus, let us consider solving the differential equation

$$\frac{d^2 f(x)}{dx^2} + f(x) = 0 \quad (11.14)$$

*Solution of one-dimensional differential equation*

over the region  $0 \leq x \leq 1$ , with the boundary conditions specified as  $f(0) = 0$  and  $f(1) = 1$ . Then we divide the region of interest  $0 \leq x \leq 1$  into  $n$  equal segments, thereby identifying  $(n + 1)$  grid points, including the two end points. The situation is illustrated in Fig. 11.3(a) for  $n = 4$ . Since the values of  $f$  at the end points 0 and 4 are specified, we need to find the values at the three interior grid points 1, 2, and 3, and hence we need to obtain a set of three algebraic equations.

Let us consider the  $k$ th grid point, where  $k = 1, 2, 3$ . Then, at that grid point,  $x = ka$ , where  $a$  is the spacing between two adjacent grid points, as shown in Fig. 12.1(b). We can approximate  $d^2f/dx^2$  at this grid point as

$$\begin{aligned} \left[ \frac{d^2f}{dx^2} \right]_k &= \left[ \frac{d^2f}{dx^2} \right]_{x=ka} \\ &\approx \frac{1}{a} \left[ \left( \frac{df}{dx} \right)_{x=(k-0.5)a} - \left( \frac{df}{dx} \right)_{x=(k+0.5)a} \right] \\ &\approx \frac{1}{a} \left[ \left( \frac{f_{k+1} - f_k}{a} \right) - \left( \frac{f_k - f_{k-1}}{a} \right) \right] \\ &= \frac{1}{a^2} (f_{k+1} - 2f_k + f_{k-1}) \end{aligned} \quad (11.15)$$

where  $f_k$  is the value of  $f$  at the  $k$ th grid point, that is, at  $x = ka$ . The right side of (11.15) is the central-difference approximation for the second derivative of  $f$  at the grid point  $k$ .

Using (11.15) and noting that here  $a$  is equal to  $\frac{1}{4}$ , we can write the finite-difference approximation for the differential equation at the  $k$ th grid point as

$$16(f_{k+1} - 2f_k + f_{k-1}) + f_k = 0$$

or

$$16f_{k-1} - 31f_k + 16f_{k+1} = 0 \quad (11.16)$$

Applying this result to the three interior grid points 1, 2, and 3, we obtain the set of three equations

$$16f_0 - 31f_1 + 16f_2 = 0$$

$$16f_1 - 31f_2 + 16f_3 = 0$$

$$16f_2 - 31f_3 + 16f_4 = 0$$

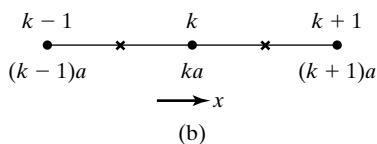
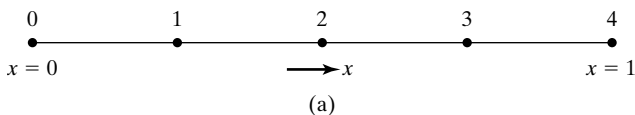


FIGURE 11.3

For the solution of one-dimensional differential equation using the finite-difference method.



Recognizing that  $f_0 = 0$  and  $f_4 = 1$ , these three equations can be arranged in matrix form as

$$\begin{bmatrix} -31 & 16 & 0 \\ 16 & -31 & 16 \\ 0 & 16 & -31 \end{bmatrix} \begin{bmatrix} f_1 \\ f_2 \\ f_3 \end{bmatrix} = \begin{bmatrix} 0 \\ 0 \\ -16 \end{bmatrix}$$

Solving, we obtain  $f_1 = 0.2943$ ,  $f_2 = 0.5702$ , and  $f_3 = 0.8109$ . An analytical solution reveals that the exact solution for  $f(x)$  is  $(\sin x)/(\sin 1)$ , which gives  $f_1 = 0.2940$ ,  $f_2 = 0.5697$ , and  $f_3 = 0.8101$ . Thus, the numerical solution is accurate to the fourth decimal place even for the number of interior grid points as small as 3.

*Solution of two-dimensional Laplace's equation*

The procedure can be extended to two-dimensional and three-dimensional differential equations. One equation of interest is the Laplace's equation (5.61). We shall consider the two-dimensional Laplace's equation in the Cartesian coordinates  $x$  and  $y$ , given by

$$\nabla^2 V = \frac{\partial^2 V}{\partial x^2} + \frac{\partial^2 V}{\partial y^2} = 0 \quad (11.17)$$

To introduce the principle behind the numerical solution of (11.17), let us suppose that we know the potentials  $V_1$ ,  $V_2$ ,  $V_3$ , and  $V_4$  at four points equidistant from a point  $P(0, 0, 0)$  and lying on mutually perpendicular axes,  $x$  and  $y$ , passing through  $P$  as shown in Fig. 11.4, and that we wish to find the potential  $V_0$  at  $P$  in terms of  $V_1$ ,  $V_2$ ,  $V_3$ , and  $V_4$ . Then we require that

$$[\nabla^2 V]_P = \left[ \frac{\partial^2 V}{\partial x^2} + \frac{\partial^2 V}{\partial y^2} \right]_{(0,0,0)} = 0 \quad (11.18)$$

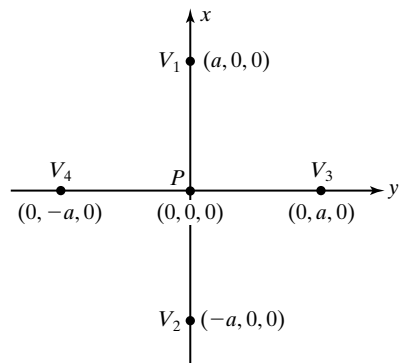


FIGURE 11.4

For illustrating the principle behind the numerical solution of Laplace's equation in two dimensions.

To solve this equation approximately for  $V_0$ , we note that

$$\begin{aligned}
 \left[ \frac{\partial^2 V}{\partial x^2} \right]_{(0,0,0)} &= \left[ \frac{\partial}{\partial x} \left( \frac{\partial V}{\partial x} \right) \right]_{(0,0,0)} \\
 &\approx \frac{1}{a} \left\{ \left[ \frac{\partial V}{\partial x} \right]_{(a/2,0,0)} - \left[ \frac{\partial V}{\partial x} \right]_{(-a/2,0,0)} \right\} \\
 &\approx \frac{1}{a} \left\{ \frac{[V]_{(a,0,0)} - [V]_{(0,0,0)}}{a} - \frac{[V]_{(0,0,0)} - [V]_{(-a,0,0)}}{a} \right\} \quad (11.19a) \\
 &= \frac{1}{a^2} [(V_1 - V_0) - (V_0 - V_2)] \\
 &= \frac{1}{a^2} (V_1 + V_2 - 2V_0)
 \end{aligned}$$

Similarly,

$$\left[ \frac{\partial^2 V}{\partial y^2} \right]_{(0,0,0)} \approx \frac{1}{a^2} (V_3 + V_4 - 2V_0) \quad (11.19b)$$

Substituting (11.19a) and (11.19b) into (11.18) and rearranging, we obtain

$$\boxed{V_0 \approx \frac{1}{4}(V_1 + V_2 + V_3 + V_4)} \quad (11.20)$$

Thus, the potential at  $P$  is approximately equal to the average of the potentials at the four equidistant points lying along mutually perpendicular axes through  $P$ . The result becomes more and more accurate as the spacing  $a$  becomes less and less. Equation (11.20) is the finite-difference approximation to (11.17) and forms the basis for its numerical solution by the finite-difference method. We shall illustrate this by means of an example.

### Example 11.3 Finite-difference method of solution of Laplace's equation in two dimensions

Let us consider four infinitely long conducting strips of equal widths, situated such that the cross section of the arrangement is a square and held at potentials  $V_a$ ,  $V_b$ ,  $V_i$ , and  $V_r$ , as shown in Fig. 11.5. Note that the corners are insulated so that the plates do not touch. By dividing the area between the conductors into a  $6 \times 6$  grid of squares, and using (11.20), we wish to find the approximate values of the potentials at the grid points by the finite-difference method.

The solution consists of obtaining a set of values for the potentials at the grid points such that the potential at each grid point is the average of the potentials at the neighboring four grid points to within a specified tolerance. Thus, if we denote the

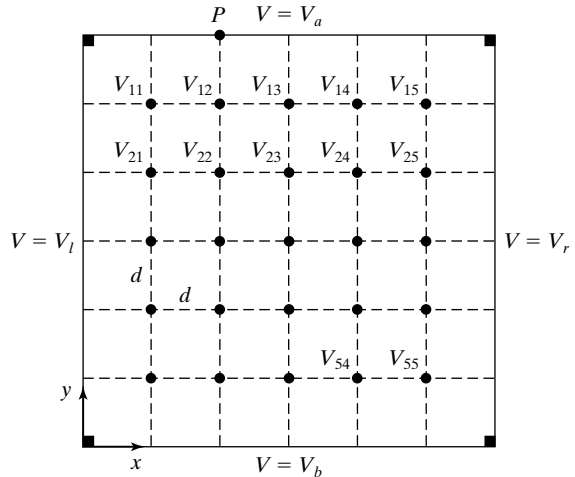


FIGURE 11.5

Cross-sectional view of an arrangement of four infinitely long conducting strips, with the region inside divided into a  $6 \times 6$  grid of squares.

potentials to be  $V_{11}, V_{12}, V_{13}, V_{14}, V_{15}, V_{21}, V_{22}, \dots, V_{55}$ , and if the specified tolerance is denoted to be  $\Delta$ , then the values of the potentials must be such that

$$|V_{11} - \frac{1}{4}(V_a + V_{12} + V_{21} + V_l)| < \Delta \quad (11.21a)$$

$$|V_{12} - \frac{1}{4}(V_a + V_{13} + V_{22} + V_{11})| < \Delta \quad (11.21b)$$

and so on. The simplest technique adaptable to computer solution is to begin with values of zero for all unknown potentials. By traversing the grid in a systematic manner, the average of the four neighboring potentials is computed for each grid point and is used to replace the potential at that grid point if that value differs from the computed average by more than  $\Delta$ . This procedure is repeated until a final set of values for the unknown potentials consistent with (11.21a), (11.21b), ... is obtained.

Let us consider some numerical values:  $V_a = 100 \text{ V}$ ,  $V_b = 0 \text{ V}$ ,  $V_l = 40 \text{ V}$ ,  $V_r = 0 \text{ V}$ , and  $\Delta = 0.01 \text{ V}$ . Then we first set all unknown potentials equal to zero. Beginning at the grid point 11 and traversing the grid rowwise, we replace the zero value for  $V_{11}$  by  $\frac{1}{4}(100 + 40 + 0 + 0)$ , or  $35 \text{ V}$ , then replace the zero value for  $V_{12}$  by  $\frac{1}{4}(100 + 35 + 0 + 0)$ , or  $33.75 \text{ V}$ , and so on. After one traversal is completed, we come back to the grid point 11 and traverse the grid again, replacing the potential value at each grid point by the average of the then-existing values of the four neighboring potentials, as necessary. This procedure is repeated until the desired set of values is obtained.

The procedure just discussed can be very conveniently carried out by using a computer program. The final set of values from the run of such a program for  $V_a = 100 \text{ V}$ ,  $V_b = 0 \text{ V}$ ,  $V_l = 40 \text{ V}$ ,  $V_r = 0 \text{ V}$ , and  $\Delta = 0.01 \text{ V}$  is shown in Fig. 11.6, which also shows the residuals, where a residual at a grid point is the absolute value of the difference between the potential at that grid point and the average of the four neighboring potentials. The residuals are shown below the potential values. It can be seen that all residuals are less than  $0.01 \text{ V}$ .

	100	100	100	100	100	
40	65.60 0.006	72.71 0.006	72.30 0.004	65.76 0.006	48.10 0.006	0
40	49.69 0.006	52.99 0.007	50.73 0.004	42.68 0.007	26.66 0.006	0
40	40.21 0.004	38.84 0.004	34.95 0.000	27.61 0.004	15.89 0.004	0
40	32.32 0.006	27.23 0.007	22.65 0.004	16.92 0.007	9.29 0.006	0
40	21.86 0.006	15.14 0.006	11.49 0.004	8.19 0.006	4.36 0.006	0
	0	0	0	0	0	

ITERATION NO. = 25  
 SOLUTION COMPLETED  
 VALUE OF DELTA ACHIEVED < = 7.423401E-03

FIGURE 11.6

Final set of values of potentials and residuals for the arrangement of Fig. 11.5, for  $V_a = 100$  V,  $V_b = 0$  V,  $V_l = 40$  V,  $V_r = 0$  V, and  $\Delta = 0.01$  V.

The method we just discussed is known as the *iteration* technique since it involves the iterative process of converging an initially assumed solution to a final one consistent with Laplace's equation in the approximate sense given by (11.20). There are several variations of the iteration technique. For example, by employing an initial guess other than zeros, a faster convergence may be achieved. The end result will, however, still be only to within the specified accuracy. Alternative to the iteration technique, one can write a set of simultaneous equations by applying (11.20) to each grid point and then solve the equations for the unknown potentials, as already illustrated for the one-dimensional case.

*Iteration  
 technique*

The solution obtained for the potentials at the grid points by any method can be used to plot approximately the equipotential lines by interpolating between grid points. An example of such plotting, also by using a computer, is shown in Fig. 11.7, which corresponds to that of  $V_a = V_l = V_b = 0$  V and  $V_r = 100$  V in Fig. 11.5, and an  $8 \times 8$  grid of squares. Figure 11.7(a) shows the computed potential values at a  $4 \times 4$  set of grid points (with the remaining grid points omitted for the sake of clarity) and the 25-V equipotential line being plotted. Figure 11.7(b) shows a complete set of equipotential lines from 0 to 100 V in steps of 10 V. Note that in Fig. 11.7(b) the 0-V equipotential line does not follow the boundary at the upper- and lower-left corners. This is because in view of the division of the region into a finite grid of squares ( $8 \times 8$  here), the solution is not influenced by the corner points; that is, the solution for the case of the 0-V conductor following the plotted 0-V line is the same as that for which it follows the original boundary.

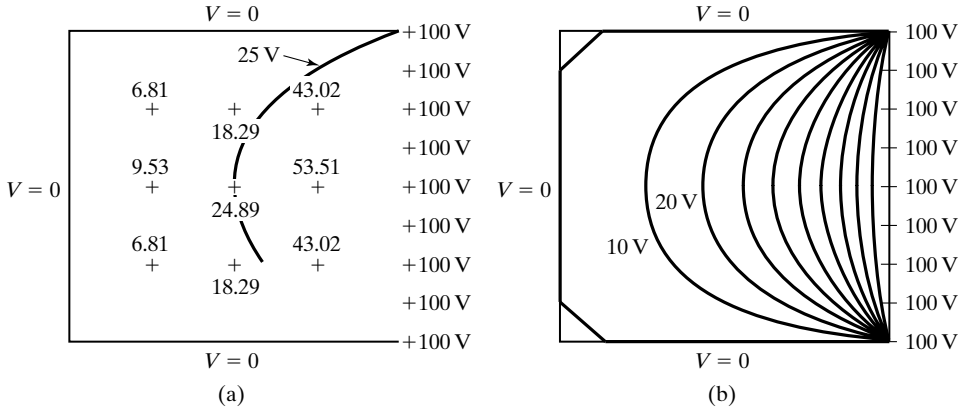


FIGURE 11.7

(a) Plotting of an equipotential line by interpolation between grid points. (b) Set of equipotential lines from 0 to 100 V in steps of 10 V.

Finally, the solution for the potentials can also be used to find approximate electric field intensities at the grid points by using the potential values to obtain approximate values of  $\partial V/\partial x$  and  $\partial V/\partial y$ . For example, in Fig. 11.5, the electric-field intensity at the grid point 12 is given approximately by

$$[\mathbf{E}]_{12} \approx \frac{V_{11} - V_{13}}{2d} \mathbf{a}_x + \frac{V_{22} - V_a}{2d} \mathbf{a}_y$$

where  $d$  is the spacing between two adjacent grid points. Similarly, the electric-field intensities at points on the conductors can be found and used to obtain the surface charge densities. For example, the surface charge density at the point  $P$  on the conductor of potential  $V_a$  and adjacent to the grid point 12 is given approximately by

$$\begin{aligned} [\rho_S]_P &\approx -\mathbf{a}_y \cdot \boldsymbol{\varepsilon} \frac{V_{12} - V_a}{d} \mathbf{a}_y \\ &= \boldsymbol{\varepsilon} \frac{V_a - V_{12}}{d} \end{aligned}$$

where  $\boldsymbol{\varepsilon}$  is the permittivity of the medium between the conductors.

**K11.2.** Finite-difference method; Solution of one-dimensional differential equation; Solution of Laplace’s equation in two dimensions; Iteration technique.

**D11.2.** Three infinitely long conductor strips are arranged such that the cross section is an isosceles triangle, as shown in Fig. 11.8. The region between the conductors is divided into a grid of points as shown in the figure, where the spacing between adjacent pairs of points is  $d$ . By writing equations consistent with (11.20)

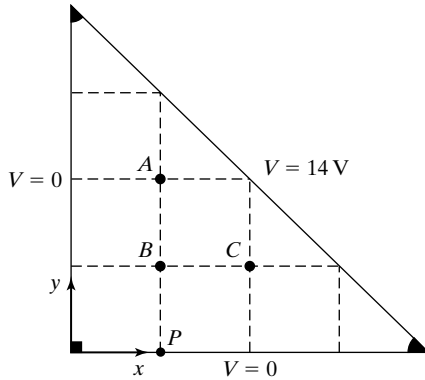


FIGURE 11.8  
For Problem D11.2.

for the potentials at the grid points  $A$ ,  $B$ , and  $C$  and solving them, find the following: **(a)** the approximate potential at the grid point  $C$ ; **(b)** the approximate electric field intensity at the grid point  $C$ ; and **(c)** the approximate surface charge density at the point  $P$ , assuming the medium between the conductors to be free space.

Ans. **(a)**  $8\text{ V}$ ; **(b)**  $-(5\mathbf{a}_x + 7\mathbf{a}_y)/d\text{ V/m}$ ; **(c)**  $-4\epsilon_0/d\text{ C/m}^2$ .

### 11.3 METHOD OF MOMENTS

When the boundaries of the physical arrangement extend to infinity, the finite-difference method cannot be used unless some approximations are made to limit the extent for the grid to be finite. Another numerical technique, known as the *method of moments*, is useful in such situations. The method of moments is commonly used to solve integral equations. An example consists of finding the charge distribution on the conductors held at known constant potentials. Thus, the problem is the inverse of the problem of finding the potential for a known charge distribution. To cast the technique in general terms, let us consider a surface charge distribution  $\rho_S(x, y, z)$  on a given surface. Then applying superposition in conjunction with the expression for the potential due to a point charge given by (5.35), the potential due to the charge distribution can be expressed as

$$V(x, y, z) = \frac{1}{4\pi\epsilon_0} \int_{\text{surface of the charge distribution}} \frac{\rho_S(x', y', z')}{R} dS' \quad (11.22)$$

where the primes denote source point coordinates. The procedure consists of dividing the surface into a finite number of subsections to approximate the integral in (11.22) by a summation and applying the equation to points on the subsections to obtain a set of linear algebraic equations. The set of equations is then inverted to obtain the desired solution. We shall illustrate the method by means of an example.

### Example 11.4 Application of method of moments to a straight wire held at a known potential

*Thin, straight wire held at known potential*

Let us consider a thin, straight wire of length  $l$  and radius  $a$  ( $\ll l$ ), as shown in Fig. 11.9(a), held at a potential of 1 V. We wish to obtain the resulting (surface) charge distribution on the wire by the method of moments.

The determination of the charge distribution by the method of moments consists of dividing the wire into a number of segments, assuming the charge density in each segment to be uniform, and setting up and solving a set of algebraic equations. For simplicity of illustration, we shall divide the wire into five equal segments numbered 1 through 5 and having surface charge densities  $\rho_{S1}, \rho_{S2}, \dots, \rho_{S5}$ . From considerations of symmetry, there are then only three unknowns, since  $\rho_{S4} = \rho_{S2}$  and  $\rho_{S5} = \rho_{S1}$ . Hence, we need three independent equations.

An equation is obtained by writing the potential at the center point of a given segment to be the superposition of the potentials at that point due to the charges in the five segments. To obtain the contribution due to a segment, we consider the cylindrical surface charge of uniform density  $\rho_{S0}$  coaxial with the  $z$ -axis and located symmetrically about the origin, as shown in Fig. 11.9(b), and compute the potential due to it at two points: (1) at the origin and (2) at a point  $(0, 0, z)$ , where  $z > d$ , using the approximation  $a \ll d$ . Case 1 is appropriate to finding the potential due to the charge in a given segment in Fig. 11.9(a) at its own center point, whereas case 2 is appropriate to finding the potential due to the charge in a given segment in Fig. 11.9(a) at the center point of another segment.

Dividing the cylindrical surface charge in Fig. 11.9(b) into a number of ring charges, one of which is shown in the figure, and using superposition, we obtain

$$\begin{aligned} [V]_{(0,0,0)} &= \int_{z'=-d}^d \int_{\phi=0}^{2\pi} \frac{\rho_{S0} a d\phi dz'}{4\pi\epsilon_0 \sqrt{a^2 + (z')^2}} \\ &= \frac{\rho_{S0} a}{2\epsilon_0} \left\{ \ln [z' + \sqrt{a^2 + (z')^2}] \right\}_{z'=-d}^d \\ &= \frac{\rho_{S0} a}{2\epsilon_0} \ln \frac{d + \sqrt{a^2 + d^2}}{-d + \sqrt{a^2 + d^2}} \end{aligned}$$

which for  $a \ll d$  reduces to

$$\begin{aligned} [V]_{(0,0,0)} &\approx \frac{\rho_{S0} a}{2\epsilon_0} \ln \frac{2d}{-d + d(1 + a^2/2d^2)} \\ &= \frac{\rho_{S0} a}{\epsilon_0} \ln \frac{2d}{a} \end{aligned} \quad (11.23a)$$

For a point  $P(0, 0, z)$ , where  $z > d$ , we can consider the cylindrical surface charge to be a line charge of density  $2\pi a\rho_{S0}$  and write

$$\begin{aligned} [V]_P &= \int_{z'=-d}^d \frac{2\pi a\rho_{S0} dz'}{4\pi\epsilon_0(z - z')} \\ &= \frac{\rho_{S0} a}{2\epsilon_0} [-\ln(z - z')]_{z'=-d}^d \\ &= \frac{\rho_{S0} a}{2\epsilon_0} \ln \frac{z + d}{z - d} \end{aligned} \quad (11.23b)$$

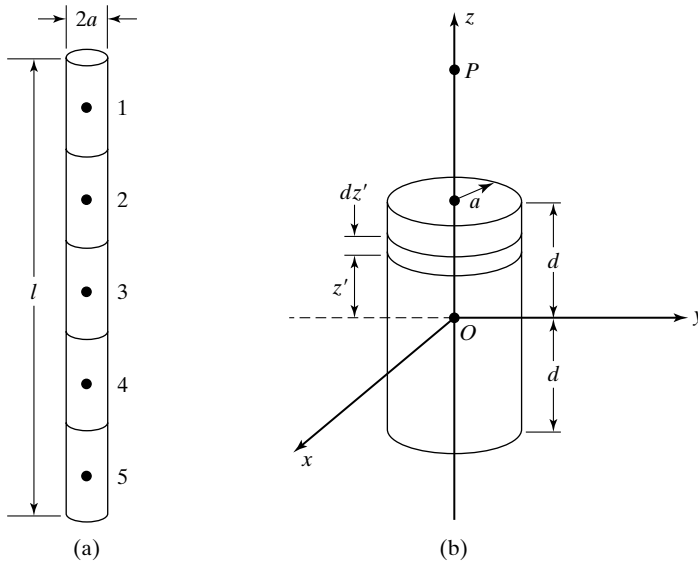


FIGURE 11.9

(a) Thin wire divided into five equal segments. (b) For the determination of the potential due to a cylindrical surface charge.

Applying (11.23a) and (11.23b) to write the equation for the potential at the center of segment 1 in Fig. 11.9(a), we obtain

$$\frac{\rho_{S1}a}{\epsilon_0} \ln \frac{l}{5a} + \frac{\rho_{S2}a}{2\epsilon_0} \ln 3 + \frac{\rho_{S3}a}{2\epsilon_0} \ln \frac{5}{3} + \frac{\rho_{S4}a}{2\epsilon_0} \ln \frac{7}{5} + \frac{\rho_{S5}a}{2\epsilon_0} \ln \frac{9}{7} = 1$$

or

$$\rho_{S1} \left( 2 \ln \frac{l}{5a} + \ln \frac{9}{7} \right) + \rho_{S2} (\ln 3 + \ln 1.4) + \rho_{S3} \ln \frac{5}{3} = \frac{2\epsilon_0}{a} \quad (11.24)$$

where we have substituted  $\rho_{S5} = \rho_{S1}$  and  $\rho_{S4} = \rho_{S2}$ . Similarly, writing the equations for the potentials at the center points of segments 2 and 3 and arranging the three equations in matrix form, we get

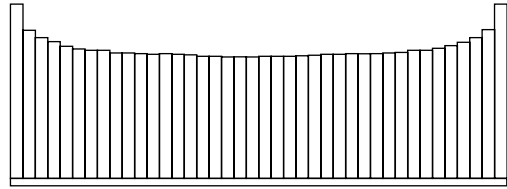
$$\begin{bmatrix} 2 \ln \frac{l}{5a} + \ln \frac{9}{7} & \ln 3 + \ln 1.4 & \ln \frac{5}{3} \\ \ln 3 + \ln 1.4 & 2 \ln \frac{l}{5a} + \ln \frac{5}{3} & \ln 3 \\ 2 \ln \frac{5}{3} & 2 \ln 3 & 2 \ln \frac{l}{5a} \end{bmatrix} \begin{bmatrix} \rho_{S1} \\ \rho_{S2} \\ \rho_{S3} \end{bmatrix} = \begin{bmatrix} \frac{2\epsilon_0}{a} \\ \frac{2\epsilon_0}{a} \\ \frac{2\epsilon_0}{a} \end{bmatrix} \quad (11.25)$$

By inverting (11.25), the solutions for  $\rho_{S1}$ ,  $\rho_{S2}$ , and  $\rho_{S3}$  can be obtained. For a numerical example, if  $l = 1$  m and  $a = 1$  mm, the values of  $\rho_{S1}$ ,  $\rho_{S2}$ , and  $\rho_{S3}$  are  $158.38\epsilon_0$ ,  $145.42\epsilon_0$ , and  $143.32\epsilon_0$ , respectively. When a larger number of segments are used, a more accurate solution is obtained for the charge distribution on the wire. For example, the result for



FIGURE 11.10

Charge distribution along a thin, straight wire of length 1 m and radius 1 mm, and held at a potential of 1 V. The height of the first rectangle is  $204\epsilon_0 \text{ C/m}^2$ .



$n = 40$  obtained by using a computer program is shown in Fig. 11.10, where the height of the first rectangle is  $204\epsilon_0 \text{ C/m}^2$ .

*Capacitance  
of a parallel-  
plate  
capacitor*

Proceeding further, we recall that in Example 5.6 we discussed the solution of Laplace's equation for the one-dimensional case of two infinite, plane, parallel, perfectly conducting plates, which may be considered an idealization of a parallel-plate capacitor with its plates having large dimensions compared to the spacing between them. We then obtained the expression for the capacitance of the arrangement per unit area of the plates. Because of the idealization, this expression is only approximate for a capacitor with finite-sized plates. It becomes less and less accurate as the size of the plates becomes less and less large for a given spacing between them, since the fringing of the field at the edges of the plates becomes more and more severe. Thus, the problem is that, in the nonideal case, the field distribution between the capacitor plates and the charge distribution on the capacitor plates are not uniform, whereas, for the ideal case, they are uniform. Hence, it is not in general possible to obtain an analytical expression for the capacitance; one has to resort to numerical or graphical techniques. The method of moments serves as a useful tool for such cases.

For an example, let us consider an arrangement in which the spacing between the plates is  $a$ , the dimensions of the plates are  $2a \times 3a$ , and from symmetry considerations, the upper plate is held at a potential of 1 V and the lower plate is held at a potential of  $-1$  V. For the purposes of illustration of the method, we shall divide each plate into a  $2 \times 3$  set of squares, as shown in Fig. 11.11, and assume that within each square, the (surface) charge density is uniform. From symmetry considerations, we then have only two unknown charge densities  $\rho_{S1}$ , and  $\rho_{S2}$ , as shown in the figure. Therefore, it is sufficient to write two independent equations. We shall do this by considering squares 1 and 2 and equating the potentials at the center points of these squares to 1 V.

To write the expression for the potential at the center point of a square due to the charge in a different square, we shall consider that charge to be a point charge at the center of the square. Thus, the potential at point 1 due to the charge in square 4 is  $\rho_{S1}a^2/4\pi\epsilon_0a$ , the potential at point 2 due to the charge in square 12 is  $-\rho_{S1}a^2/4\pi\epsilon_0(\sqrt{3}a)$ , and so on. To write the expression for the potential at the center point of a square due to the charge in that square, we shall use the result given in Problem P5.11. For example, the potential at point 1 due

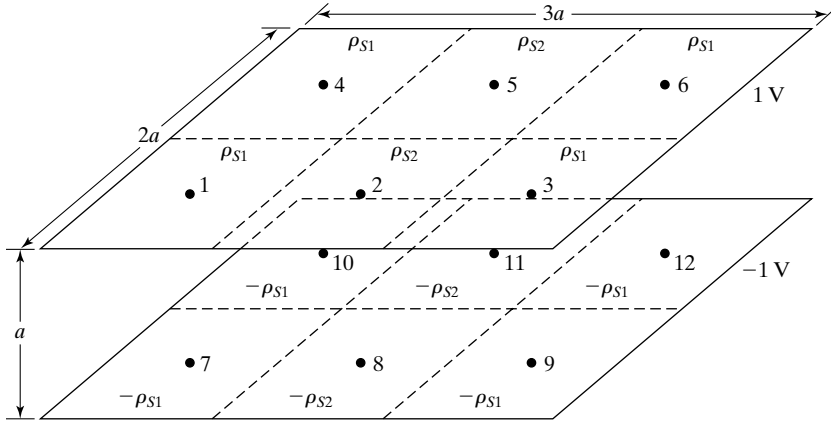


FIGURE 11.11

For finding the capacitance of a parallel-plate capacitor by the method of moments.

to the charge in square 1 is  $(\rho_{S1}a/\pi\epsilon_0) \ln(1 + \sqrt{2})$ . Proceeding in this manner, we obtain the two equations to be

$$\begin{aligned} \frac{\rho_{S1}a}{\pi\epsilon_0} \ln(1 + \sqrt{2}) + \frac{\rho_{S1}a^2}{4\pi\epsilon_0} \left( \frac{1}{2a} + \frac{1}{a} + \frac{1}{\sqrt{5}a} - \frac{1}{a} - \frac{1}{\sqrt{5}a} - \frac{1}{\sqrt{2}a} - \frac{1}{\sqrt{6}a} \right) \\ + \frac{\rho_{S2}a^2}{4\pi\epsilon_0} \left( \frac{1}{a} + \frac{1}{\sqrt{2}a} - \frac{1}{\sqrt{2}a} - \frac{1}{\sqrt{3}a} \right) = 1 \end{aligned} \quad (11.26a)$$

$$\begin{aligned} \frac{\rho_{S2}a}{\pi\epsilon_0} \ln(1 + \sqrt{2}) + \frac{\rho_{S1}a^2}{4\pi\epsilon_0} \left( \frac{2}{a} + \frac{2}{\sqrt{2}a} - \frac{2}{\sqrt{2}a} - \frac{2}{\sqrt{3}a} \right) \\ + \frac{\rho_{S2}a^2}{4\pi\epsilon_0} \left( \frac{1}{a} - \frac{1}{a} - \frac{1}{\sqrt{2}a} \right) = 1 \end{aligned} \quad (11.26b)$$

or

$$2.9101\rho_{S1} + 0.4226\rho_{S2} = \frac{4\pi\epsilon_0}{a} \quad (11.27a)$$

$$0.8453\rho_{S1} + 2.8184\rho_{S2} = \frac{4\pi\epsilon_0}{a} \quad (11.27b)$$

Solving (11.27a) and (11.27b) for  $\rho_{S1}$  and  $\rho_{S2}$ , we obtain  $\rho_{S1} = 3.8378\epsilon_0/a$  and  $\rho_{S2} = 3.3075\epsilon_0/a$ . The magnitude of charge on either plate is then equal to  $(4a^2 \times 3.8378\epsilon_0/a + 2a^2 \times 3.3075\epsilon_0/a)$ , or  $21.9662\epsilon_0a$ . Finally, noting that the potential difference between the plates is 2 V, the capacitance can be computed to be  $10.983\epsilon_0a$ . A more accurate result can be obtained by dividing each

plate into a larger number of squares, but it is instructive to compare the value just obtained with the value of  $6\epsilon_0 a$ , which follows from the application of  $C = \epsilon_0 A/d$ , where  $A$  is the area of the plates, and  $d$  is the spacing between the plates.

- K11.3.** Method of moments; Thin, straight wire held at known potential; Determination of charge distribution; Parallel-plate capacitor; Determination of capacitance.
- D11.3.** For the problem of Example 11.4, consider that to compute the potential at the center of a given segment due to the charge in another segment, the charge in that segment can be assumed to be a point charge at the center of that segment. Modify the formulation to obtain the new matrix equation in the place of (11.25) and find the values of  $\rho_{S1}$ ,  $\rho_{S2}$ , and  $\rho_{S3}$ , for  $l = 1$  m and  $a = 1$  mm.  
*Ans.*  $159.48\epsilon_0$  C/m<sup>2</sup>;  $147.94\epsilon_0$  C/m<sup>2</sup>;  $145.77\epsilon_0$  C/m<sup>2</sup>.
- D11.4.** Consider a parallel-plate capacitor having square-shaped plates of sides  $a$  and spacing  $a$  between the plates. Find the following: **(a)** the capacitance of the capacitor if fringing of fields at the edges of the plates is neglected; **(b)** the capacitance by using the method of moments, considering each plate as one square; and **(c)** the capacitance by dividing each plate into a  $2 \times 2$  set of squares and using the method of moments. Assume free space for the dielectric.  
*Ans.* **(a)**  $\epsilon_0 a$ ; **(b)**  $2.488\epsilon_0 a$ ; **(c)**  $2.8367\epsilon_0 a$ .

## 11.4 DETERMINATION OF TRANSMISSION-LINE PARAMETERS

In this section, we shall illustrate the application of the numerical methods introduced in the previous two sections for the determination of transmission-line parameters, by means of two examples.

---

### Example 11.5 Determination of parallel-strip line parameters by using method of moments

*Parallel-strip line*

The parallel-strip line is the same as the parallel-plate line (see Fig. 6.2) without the imposition of the approximation  $d/w \ll 1$ , such that fringing of fields can not be neglected. We wish to find the capacitance per unit length and hence the characteristic impedance of the parallel-strip line embedded in a homogeneous medium (which we shall assume here to be free space) for the case of  $d = w$ , by using the method of moments.

The procedure for the application of method of moments to find the capacitance per unit length of a parallel-strip line is similar to that used for finding the capacitance of a parallel-plate capacitor in Section 11.3. Thus, let us consider the cross-sectional view of the parallel-strip line and divide each conductor into  $2n$  substrips, as shown in Fig. 11.12 for  $n = 3$ , and assume the charge density in each substrip to be uniform. From symmetry considerations, we can apply a potential of 1 V to one of the conductors and  $-1$  V to the other conductor. Also from symmetry considerations, there are only  $n(= 3)$  unknown charge densities to be determined, namely, the charge densities associated with the substrips in one half of one of the conductors. Thus, we need to write a set of  $n(= 3)$  independent equations for the  $n(= 3)$  unknown charge densities. To do this, we consider pairs of substrips  $11'$ ,  $22'$ ,  $\dots$ , situated opposite to each other, and we write the expression

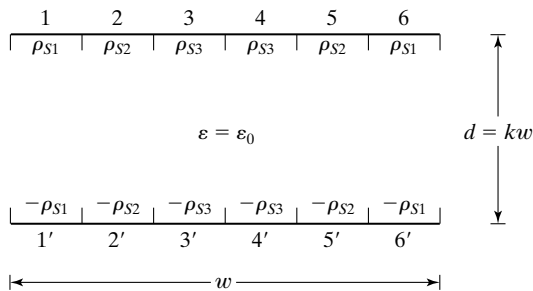


FIGURE 11.12

Division of the conductors of a parallel-strip line into substrips.

for the potential difference between the center points of each pair and set that equal to  $2V$ . The expression for the potential difference between the center points of a given pair is the sum of the contributions to the potential difference from all  $2n (= 6)$  pairs. To obtain the contribution from a given pair, we make use of the result given in Problem P5.12 for the potential difference between two points due to an infinitely long strip of uniform surface charge density. For example, let us consider the potential difference between the center points of 1 and 1'. Then the contribution to it from the pair of substrips 1 and 1' is

$$\frac{\rho_{S1}}{2\pi\epsilon_0} \left[ \frac{w}{6} \ln \frac{(w/12)^2 + d^2}{(w/12)^2} + 4d \tan^{-1} \frac{w}{12d} \right]$$

whereas the contribution from the pair of substrips 2 and 2' is

$$\frac{\rho_{S2}}{2\pi\epsilon_0} \left[ \frac{w}{4} \ln \frac{(w/4)^2 + d^2}{(w/4)^2} - \frac{w}{12} \ln \frac{(w/12)^2 + d^2}{(w/12)^2} + 2d \left( \tan^{-1} \frac{w}{4d} - \tan^{-1} \frac{w}{12d} \right) \right]$$

Writing contributions in this manner and adding appropriately, we obtain the matrix equation for the three unknown charge densities  $\rho_{S1}$ ,  $\rho_{S2}$ , and  $\rho_{S3}$  for the case of  $d = w$ , that is,  $k = 1$ , as given by

$$\begin{bmatrix} 1.311 & 0.815 & 0.658 \\ 0.815 & 1.432 & 1.005 \\ 0.658 & 1.005 & 1.779 \end{bmatrix} \begin{bmatrix} \rho_{S1} \\ \rho_{S2} \\ \rho_{S3} \end{bmatrix} = \begin{bmatrix} 4\pi\epsilon_0/w \\ 4\pi\epsilon_0/w \\ 4\pi\epsilon_0/w \end{bmatrix}$$

so that

$$\begin{aligned} \rho_{S1} &= \frac{6.0854\epsilon_0}{w} \text{ C/m}^2 \\ \rho_{S2} &= \frac{3.2062\epsilon_0}{w} \text{ C/m}^2 \\ \rho_{S3} &= \frac{3.003\epsilon_0}{w} \text{ C/m}^2 \end{aligned}$$

The magnitude of the charge per unit length on either conductor is

$$(w/3) \times (\rho_{S1} + \rho_{S2} + \rho_{S3})(1) = 4.098\epsilon_0 C$$

Thus, the capacitance per unit length is given by

$$\mathcal{C} = \frac{4.0982\epsilon_0}{2} = 2.0491\epsilon_0 \text{ F/m}$$

Finally, the characteristic impedance of the parallel-strip line for the case of  $d = w$  is  $\sqrt{\mu_0\epsilon_0}/2.0491\epsilon_0$ , or  $183.98 \Omega$ . For larger values of  $n$ , the solution can be carried out by using a computer program. For example, for  $d = w = 1 \text{ cm}$ , and  $n = 10$ , the values of  $\mathcal{C}$  and  $Z_0$  can be computed to be  $18.5252 \text{ pF/m}$  and  $179.9352 \Omega$ , respectively.

**Example 11.6 Determination of enclosed-microstrip line parameters by finite-difference method**

*Enclosed-microstrip line*

When the bottom conductor of the microstrip line of Fig. 6.5 is extended so as to surround the top conductor, we get the enclosed-microstrip line, as shown by the cross-sectional view in Fig. 11.13. Here we assume a square cross section for the line by the outer conductor and wish to determine the propagation parameters for the line by using the finite-difference method to find the values of capacitance per unit length with and without the dielectric substrate in place, as required by (6.25a) and (6.25b), in view of the inhomogeneity.

For purposes of illustration, we divide the region inside the outer conductor into a  $6 \times 6$  set of squares with the grid points identified as  $(i, j)$ , where  $i$  is the row number (1 to 5 from top to bottom), and  $j$  is the column number (1 to 5 from left to right). We place the inner conductor along the line from grid point (4, 2) to grid point (4, 4) so that the region below row 4 is dielectric substrate (relative permittivity  $\epsilon_R$ ), and the region above row 4 is free space. We further assume the inner conductor to be kept at 10 V and the outer conductor at 0 V, and apply the iteration procedure, illustrated in Example 11.3 to compute the potentials at the grid points not on the conductors. We note, however, that in view of the inhomogeneity when the dielectric substrate is in place, the modified

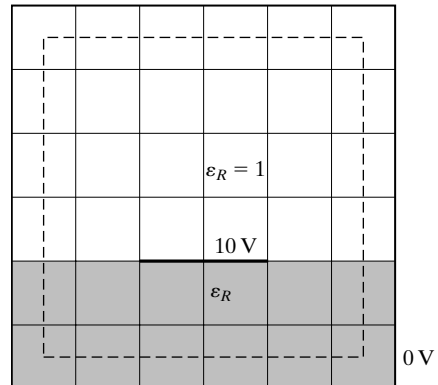


**FIGURE 11.13** Division of the region between the conductors of an enclosed-microstrip line into a set of squares.

form of (11.20) given by (see Problem P11.8)

$$V_0 \approx \frac{V_1 + \epsilon_r V_2}{2(1 + \epsilon_r)} + \frac{V_3 + V_4}{4} \tag{11.28}$$

needs to be used. Thus, the procedure consists of the following steps:

- (a) With the dielectric substrate in place, find the solution for the potentials at the grid points not on the conductors, consistent with (11.28) to within a specified tolerance ( $\Delta$ ) assumed here to be 0.01 V. Find the magnitude of the charge per unit length along the conductors by applying Gauss' law in integral form to a surface having as the cross section the contour that passes through the center points of the squares adjacent to the outer conductor, as shown in Fig. 11.13. Find the capacitance per unit length ( $\mathcal{C}$ ).
- (b) With the dielectric replaced by free space, repeat step (a) to obtain the capacitance per unit length ( $\mathcal{C}_0$ ).
- (c) Find  $Z_0$  and  $v_p$  by using (6.25a) and (6.25b), respectively.

The solution just outlined can be carried out by using a computer program. The final set of values for the potentials obtained from the run of such a program for the specific arrangement of Fig. 11.13 for  $\epsilon_R = 10$ , as well as the results for  $\mathcal{C}$ ,  $\mathcal{C}_0$ ,  $Z_0$ , and  $v_p$ , are shown in Fig. 11.14. The upper rows of potential values at the interior grid points correspond to the case of the dielectric substrate in place and the lower rows correspond to the case of the dielectric replaced by free space.

0	0	0	0	0	0	0
0	0.69	1.23	1.43	1.23	0.69	0
	0.69	1.24	1.44	1.24	0.69	
0	1.53	2.84	3.27	2.84	1.53	0
	1.54	2.85	3.28	2.85	1.54	
0	2.58	5.34	5.99	5.34	2.58	0
	2.63	5.36	6.00	5.36	2.63	
0	3.47	10.00	10.00	10.00	3.47	0
	3.64	10.00	10.00	10.00	3.64	
0	1.89	4.10	4.55	4.10	1.89	0
	1.93	4.12	4.55	4.12	1.94	
0	0	0	0	0	0	0

FIGURE 11.14

Final set of values for the potentials and the results for  $\mathcal{C}$ ,  $\mathcal{C}_0$ ,  $Z_0$ , and  $v_p$  for the enclosed-microstrip line of Fig. 11.13 for  $\epsilon_R = 10$ .

C = 226.4795 PF/m      C0 = 37.85039 PF/m  
 Z0 = 36.00221 OHMS  
 VP = 1.226428E+08 M/S

- K11.4.** Parallel-strip line; Method of moments; Enclosed-microstrip line; Finite-difference method.
- D11.5.** For the parallel-strip line of Fig. 11.12, find the following for  $d = w$ : **(a)** the contribution to the potential difference between the center points of substrips 2 and 2' from the pair of substrips 2 and 2'; **(b)** the contribution to the potential difference between the center points of substrips 2 and 2' from the pair of substrips 5 and 5'; and **(c)** the contribution to the potential difference between the center points of substrips 1 and 1' from the pair of substrips 6 and 6'.

*Ans.* **(a)**  $0.1849\rho_{S2}w/\epsilon_0$ ; **(b)**  $0.043\rho_{S2}w/\epsilon_0$ ; **(c)**  $0.0238\rho_{S1}w/\epsilon_0$ .

## 11.5 SOLUTION BY FIELD MAPPING

### *Field mapping*

For a line with arbitrary cross section and involving a homogeneous dielectric, an approximate value of  $\mathcal{C}$ , and hence of  $Z_0$ , can be determined by constructing a *field map*, that is, a graphical sketch of the direction lines of the electric field and associated equipotential lines between the conductors. To illustrate this, let us consider the cross section shown in Fig. 11.15. Assuming that the inner conductor is positive with respect to the outer conductor, we can draw the field map from the following considerations. (1) The electric field lines originate on the inner conductor and normal to it and terminate on the outer conductor and normal to it, since the tangential component of the electric field on the conductor surface must be zero. (2) The equipotential lines must be everywhere perpendicular to the electric field lines. Thus, suppose that we start with the inner conductor and draw several lines normal to it at several points on the surface, as shown in Fig. 11.15(b). We can then draw a curved line displaced from the conductor surface and perpendicular everywhere to the electric-field lines of Fig. 11.15(b), as shown in Fig. 11.15(c). This contour represents an equipotential line and forms the basis for further extension of the electric-field lines, as shown in Fig. 11.15(d). A second equipotential line can then be drawn so that it is everywhere perpendicular to the extended electric-field lines, and the procedure is continued until the entire cross section between the conductors is filled with two sets of orthogonal contours, as shown in Fig. 11.15(e), thereby resulting in a field map made up of curvilinear rectangles. For the actual, time-varying case, the magnetic-field lines are the same as the equipotential lines and the field map represents a sketch of the direction lines of electric and magnetic fields between the conductors.

By drawing the field lines with very small spacings, we can make the rectangles so small that each of them can be considered to be the cross section of a parallel-plate line. If we now replace the equipotential lines by perfect conductors, since it does not violate any boundary condition, it can be seen that the arrangement can be viewed as the parallel combination, in the angular direction, of  $m$  number of series combinations of  $n$  number of parallel-plate lines in the radial direction, where  $m$  is the number of rectangles in the angular direction,

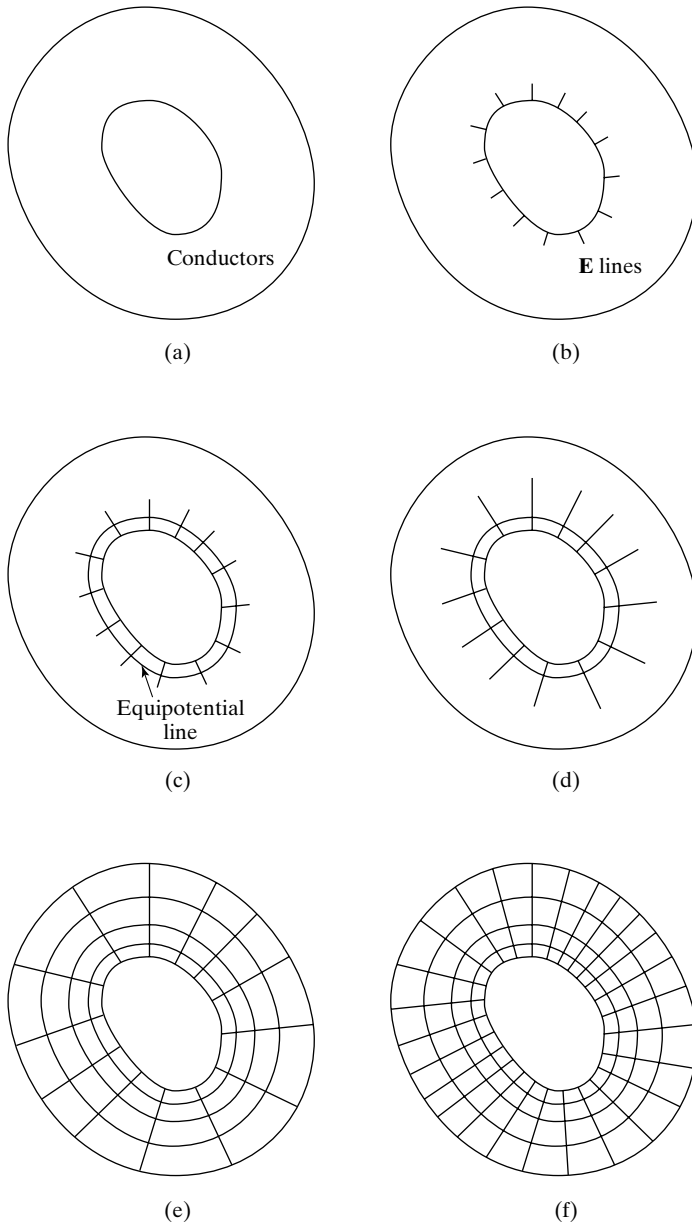


FIGURE 11.15

For illustrating the construction of a field map for a transmission line of arbitrary cross section.

that is, along a magnetic-field line, and  $n$  is the number of rectangles in the radial direction, that is, along an electric field line. If  $Q_1, Q_2, \dots, Q_m$  are the charges per unit length associated with the angular direction and  $V_1, V_2, \dots, V_n$  are the potential differences associated with the radial direction, the capacitance per



unit length of the line is given by

$$\begin{aligned}
 \mathcal{C} &= \frac{Q}{V} = \frac{Q_1 + Q_2 + \cdots + Q_m}{V_1 + V_2 + \cdots + V_n} \\
 &= \frac{1}{\frac{V_1}{Q_1} + \frac{V_2}{Q_1} + \cdots + \frac{V_n}{Q_1}} \\
 &\quad + \frac{1}{\frac{V_1}{Q_2} + \frac{V_2}{Q_2} + \cdots + \frac{V_n}{Q_2}} + \cdots + \frac{1}{\frac{V_1}{Q_m} + \frac{V_2}{Q_m} + \cdots + \frac{V_n}{Q_m}} \\
 &= \sum_{i=1}^m \frac{1}{\sum_{j=1}^n \frac{V_j}{Q_i}} \\
 &= \sum_{i=1}^m \frac{1}{\sum_{j=1}^n \mathcal{C}_{ij}}
 \end{aligned}$$

where  $\mathcal{C}_{ij} = Q_i/V_j$  is the capacitance per unit length corresponding to the rectangle  $ij$ . The simplicity of the field mapping technique lies in the fact that if the map consists entirely of curvilinear squares (a curvilinear rectangle becomes a curvilinear square if a circle can be inscribed in it), all  $\mathcal{C}_{ij}$  are approximately equal to  $\varepsilon$ , and we obtain the simple formula

$$\mathcal{C} \approx \varepsilon \frac{m}{n} \quad (11.29)$$

and hence

$$\begin{aligned}
 Z_0 &= \frac{\sqrt{\mu\varepsilon}}{\mathcal{C}} \\
 &\approx \frac{n}{m}
 \end{aligned} \quad (11.30)$$

Thus, the determination of  $Z_0$  consists of sketching a field map consisting of curvilinear squares, as shown in Fig. 11.15(f), counting the number of squares in each direction and substituting these values in (11.29). For the rough sketch of Fig. 11.15(f),  $m = 26$  and  $n = 4$ , so that  $Z_0 \approx 0.154\eta$ .

**K11.5.** Field mapping; Curvilinear squares.

**D11.6.** Two lossless transmission lines 1 and 2 have nonmagnetic ( $\mu = \mu_0$ ), homogeneous perfect dielectrics of  $\varepsilon_1 = 2.25\varepsilon_0$  and  $\varepsilon_2 = 4\varepsilon_0$ , respectively. The values of

the ratio  $m/n$  corresponding to their curvilinear square field maps are 4 and 5 for lines 1 and 2, respectively. Find (a)  $v_{p1}/v_{p2}$ , (b)  $\epsilon_1/\epsilon_2$ , and (c)  $Z_{01}/Z_{02}$ , where the subscripts 1 and 2 denote lines 1 and 2, respectively.

Ans. (a) 4/3; (b) 0.45; (c) 5/3.

## 11.6 FINITE-ELEMENT METHOD

The finite-element method, a general technique for solving differential equations, was first developed by structural engineers for the analysis of stresses and strains in complex systems. It was not until 1968 that its applications to the solution of electromagnetic-field problems were initiated. Unlike the finite-difference method, which provides solutions at an array of grid points in the region of interest, the finite-element method provides solution over the entire region of interest. Furthermore, it is difficult to apply the finite-difference method to regions having irregularly shaped boundaries, whereas the finite-element method is particularly suitable for such regions. However, the finite-element method in its precise form is elaborate and we shall here present only an introduction by considering the early simple approach.

The basic concept of the finite-element method is that although the behavior of a function may be complex when viewed over a large region, a simple approximation may be sufficient for a small subregion. The total region is divided into a number of nonoverlapping subregions called finite elements. Within each element, the function of interest is approximated by an algebraic expression, and where the adjoining elements overlap, the algebraic representations must agree to provide continuity of the function. The equations to be solved are derived not directly from the differential equations that govern the function, but from the minimization of an integral-type functional such as the electric energy in the case of the electric potential. The solution procedure in this manner consists essentially of four steps: (1) discretizing the region of interest into the finite elements, (2) deriving the governing equations for the individual finite elements, (3) relating the individual finite elements to the assembly of the elements, and (4) obtaining and solving the system of equations for the potentials. We shall describe these steps in the context of finding the solution for the two-dimensional Laplace's equation in Cartesian coordinates  $x$  and  $y$ , given by (11.16), and then illustrate by means of an example.

*Solution procedure*

**1. Discretization of region into finite elements.** In two dimensions, the finite elements are usually polygons, the simplest of which are triangles and quadrilaterals. We shall confine our presentation to triangles to keep the analysis simple. Figure 11.16 shows an example in which a region is divided into five triangular elements, with a total of seven nodes. The most common type of expression for  $V$  within an element is a polynomial expansion. For a triangular element, it is given by

$$V_e(x, y) = a + bx + cy \quad (11.31)$$

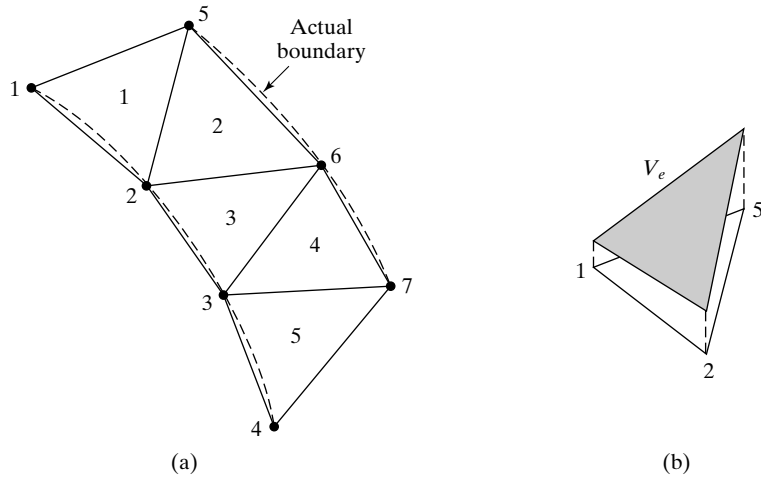


FIGURE 11.16

(a) Discretization of a region into triangular finite elements. (b) Linear variation of potential within a triangular finite element.

where the subscript  $e$  denotes element. Note that this represents linear variation of potential within the element, as shown, for example, in Fig. 11.16(b) for one element. Also, this approximation is the same as assuming that the electric field is uniform within the element, since

$$\mathbf{E} = -\nabla V_e = -(b\mathbf{a}_x + c\mathbf{a}_y) \quad (11.32)$$

**2. Equations governing the elements.** Let us consider a typical element shown in Fig. 11.17. Using (12.18), we can then express the potentials  $V_{e1}$ ,  $V_{e2}$ , and  $V_{e3}$  at nodes 1, 2, and 3, respectively, as

$$V_{e1} = a + bx_1 + cy_1 \quad (11.33a)$$

$$V_{e2} = a + bx_2 + cy_2 \quad (11.33b)$$

$$V_{e3} = a + bx_3 + cy_3 \quad (11.33c)$$

from which we can write

$$\begin{aligned} \begin{bmatrix} a \\ b \\ c \end{bmatrix} &= \begin{bmatrix} 1 & x_1 & y_1 \\ 1 & x_2 & y_2 \\ 1 & x_3 & y_3 \end{bmatrix}^{-1} \begin{bmatrix} V_{e1} \\ V_{e2} \\ V_{e3} \end{bmatrix} \\ &= \frac{1}{2A} \begin{bmatrix} (x_2y_3 - x_3y_2) & (x_3y_1 - x_1y_3) & (x_1y_2 - x_2y_1) \\ (y_2 - y_3) & (y_3 - y_1) & (y_1 - y_2) \\ (x_3 - x_2) & (x_1 - x_3) & (x_2 - x_1) \end{bmatrix} \begin{bmatrix} V_{e1} \\ V_{e2} \\ V_{e3} \end{bmatrix} \end{aligned} \quad (11.34)$$

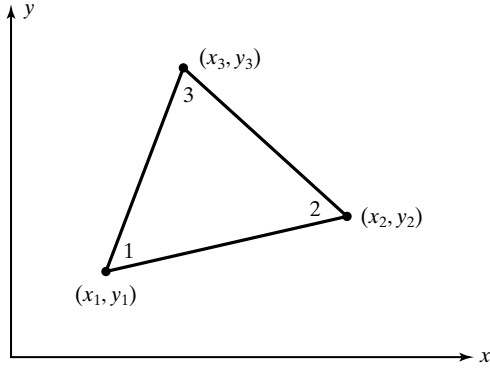


FIGURE 11.17  
A typical triangular finite element for setting up the equations governing the element.

where

$$\begin{aligned}
 A &= \frac{1}{2} \begin{vmatrix} 1 & x_1 & y_1 \\ 1 & x_2 & y_2 \\ 1 & x_3 & y_3 \end{vmatrix} \\
 &= \frac{1}{2} [(x_2 - x_1)(y_3 - y_1) - (x_3 - x_1)(y_2 - y_1)]
 \end{aligned}
 \tag{11.35}$$

is the area of the element. Note that for  $A$  to be positive, the nodes need to be numbered counterclockwise as in Fig. 11.17.

Proceeding further, we have, by substituting (11.34) into (11.31)

$$V_e = \frac{1}{2A} [1 \quad x \quad y] \begin{bmatrix} (x_2y_3 - x_3y_2) & (x_3y_1 - x_1y_3) & (x_1y_2 - x_2y_1) \\ (y_2 - y_3) & (y_3 - y_1) & (y_1 - y_2) \\ (x_3 - x_2) & (x_1 - x_3) & (x_2 - x_1) \end{bmatrix} \begin{bmatrix} V_{e1} \\ V_{e2} \\ V_{e3} \end{bmatrix}
 \tag{11.36}$$

or

$$V_e = \sum_{i=1}^3 \alpha_i(x, y) V_{ei}
 \tag{11.37}$$

where

$$\alpha_1 = \frac{1}{2A} [(x_2y_3 - x_3y_2) + (y_2 - y_3)x + (x_3 - x_2)y]
 \tag{11.38a}$$

$$\alpha_2 = \frac{1}{2A} [(x_3y_1 - x_1y_3) + (y_3 - y_1)x + (x_1 - x_3)y]
 \tag{11.38b}$$

$$\alpha_3 = \frac{1}{2A} [(x_1y_2 - x_2y_1) + (y_1 - y_2)x + (x_2 - x_1)y]
 \tag{11.38c}$$

The quantities  $\alpha_i$  are called the shape functions.

*Functional for solution of Laplace's equation*

Now, for the solution of Laplace's equation in two dimensions for the electric potential, the functional to be minimized is the electric energy per unit length normal to the two dimensions, that is,

$$W = \int \frac{1}{2} \epsilon |\mathbf{E}|^2 dS \tag{11.39}$$

over the region of interest. For the element under consideration, this is given by

$$\begin{aligned} W_e &= \int_{\text{area of } e} \frac{1}{2} \epsilon |\mathbf{E}|^2 dS \\ &= \frac{1}{2} \int_A \epsilon |\nabla V_e|^2 dS \\ &= \frac{1}{2} \epsilon \int_A (\nabla V_e \cdot \nabla V_e) dS \\ &= \frac{1}{2} \epsilon \int_A \left( \sum_{i=1}^3 V_{ei} \nabla \alpha_i \cdot \sum_{i=1}^3 V_{ei} \nabla \alpha_i \right) dS \\ &= \frac{1}{2} \epsilon \sum_{i=1}^3 \sum_{j=1}^3 V_{ei} \left( \int_A \nabla \alpha_i \cdot \nabla \alpha_j dS \right) V_{ej} \end{aligned} \tag{11.40}$$

where we have used (11.37). We now define

$$C_{ij}^{(e)} = \int_A (\nabla \alpha_i \cdot \nabla \alpha_j) dS \tag{11.41}$$

so that we can write (11.40) as

$$W_e = \frac{1}{2} \epsilon [V_e]^T [C^{(e)}] [V_e] \tag{11.42}$$

where

$$[V_e] = \begin{bmatrix} V_{e1} \\ V_{e2} \\ V_{e3} \end{bmatrix} \tag{11.43a}$$

$$[V_e]^T = [V_{e1} \quad V_{e2} \quad V_{e3}] = \text{transpose of } [V_e] \tag{11.43b}$$

and

$$[C^{(e)}] = \begin{bmatrix} C_{11}^{(e)} & C_{12}^{(e)} & C_{13}^{(e)} \\ C_{21}^{(e)} & C_{22}^{(e)} & C_{23}^{(e)} \\ C_{31}^{(e)} & C_{32}^{(e)} & C_{33}^{(e)} \end{bmatrix} \tag{11.43c}$$

The matrix  $[C^{(e)}]$  is known as the *element coefficient matrix*. Substituting (11.38a)–(11.38c) into (11.41) and evaluating, we obtain

$$C_{11}^{(e)} = \frac{1}{4A}[(y_2 - y_3)^2 + (x_2 - x_3)^2] \quad (11.44a)$$

$$C_{12}^{(e)} = \frac{1}{4A}[(y_2 - y_3)(y_3 - y_1) + (x_2 - x_3)(x_3 - x_1)] \quad (11.44b)$$

$$C_{13}^{(e)} = \frac{1}{4A}[(y_2 - y_3)(y_1 - y_2) + (x_2 - x_3)(x_1 - x_2)] \quad (11.44c)$$

$$C_{21}^{(e)} = C_{12}^{(e)} \quad (11.44d)$$

$$C_{22}^{(e)} = \frac{1}{4A}[(y_3 - y_1)^2 + (x_3 - x_1)^2] \quad (11.44e)$$

$$C_{23}^{(e)} = \frac{1}{4A}[(y_3 - y_1)(y_1 - y_2) + (x_3 - x_1)(x_1 - x_2)] \quad (11.44f)$$

$$C_{31}^{(e)} = C_{13}^{(e)} \quad (11.44g)$$

$$C_{32}^{(e)} = C_{23}^{(e)} \quad (11.44h)$$

$$C_{33}^{(e)} = \frac{1}{4A}[(y_1 - y_2)^2 + (x_1 - x_2)^2] \quad (11.44i)$$

Note that  $\sum_{i=1}^3 C_{ij}^{(e)}$ , that is, the sum of each row of  $[C^{(e)}]$ , and  $\sum_{j=1}^3 C_{ij}^{(e)}$ , that is, the sum of each column of  $[C^{(e)}]$ , are zero.

**3. Relating the individual elements to the assembly.** Proceeding further, we consider the assembly of all elements in the region of interest to write the expression for the total energy in the region. This is given by

$$W = \sum_{e=1}^n W_e = \frac{1}{2} \varepsilon [V]^T [C] [V] \quad (11.45)$$

where

$$[V] = \begin{bmatrix} V_1 \\ V_2 \\ V_3 \\ \vdots \\ V_n \end{bmatrix} \quad (11.46)$$

is the column matrix of the potentials at the nodes,  $[V]^T$  is the transpose of  $[V]$ , and  $[C]$ , which is known as the *global coefficient matrix*, is the matrix resulting from the assemblage of the individual element coefficient matrices.

To illustrate the determination of  $[C]$ , let us consider the assembly of three elements shown in Fig. 11.18. For each element, the node numbers 1, 2, and 3 are indicated inside the triangle in the counterclockwise sense. These are called *local nodes*. The nodes for the assembly, which are called *global nodes*,

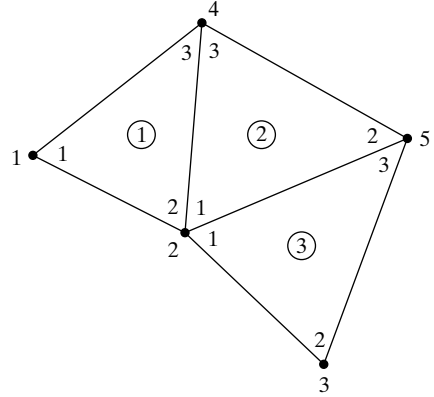


FIGURE 11.18 An assembly of three triangular finite elements, for relating the individual elements to the assembly.

are indicated at the vertices outside the assembly. The element numbers are circumscribed by circles. Since there are five global nodes,  $[C]$  is a  $5 \times 5$  matrix as given by

$$[C] = \begin{bmatrix} C_{11} & C_{12} & C_{13} & C_{14} & C_{15} \\ C_{21} & C_{22} & C_{23} & C_{24} & C_{25} \\ C_{31} & C_{32} & C_{33} & C_{34} & C_{35} \\ C_{41} & C_{42} & C_{43} & C_{44} & C_{45} \\ C_{51} & C_{52} & C_{53} & C_{54} & C_{55} \end{bmatrix} \quad (11.47)$$

The global matrix  $[C]$  is not to be confused with the element matrices  $[C^{(e)}]$ . For triangular elements, all element matrices are  $3 \times 3$ , whereas the global matrix has the size  $n \times n$ .

Since the total energy as expressed in (11.45) is the sum of the energies in the three individual elements, and since the potential distribution must be continuous across the boundaries of pairs of adjacent elements, the elements of  $[C]$  are related to the elements of the individual matrices  $[C^{(e)}]$ . Thus, for example, since global node 1 belongs to element 1 only and is the same as the local node 1,

$$C_{11} = C_{11}^{(1)}$$

Since global node 2 belongs to all three elements and is the same as local node 2 for element 1, local node 1 for element 2, and local node 1 for element 3,

$$C_{22} = C_{22}^{(1)} + C_{11}^{(2)} + C_{11}^{(3)}$$

Similarly,

$$\begin{aligned} C_{33} &= C_{22}^{(3)} \\ C_{44} &= C_{33}^{(1)} + C_{33}^{(2)} \\ C_{55} &= C_{22}^{(2)} + C_{33}^{(2)} \end{aligned}$$

The global link 12 is the same as the local link 12 for element 1. Hence,

$$C_{12} = C_{12}^{(1)}$$

The global link 23 is the same as the local link 12 for element 3. Hence,

$$C_{23} = C_{12}^{(3)}$$

The global link 24 is common to elements 1 and 2, and is the same as the local link 23 for element 1 and the local link 13 for element 2. Therefore,

$$C_{24} = C_{23}^{(1)} + C_{13}^{(2)}$$

Similarly,

$$C_{25} = C_{25}^{(2)} + C_{13}^{(3)}$$

Since there is no coupling between global nodes 1 and 3,

$$C_{13} = 0$$

In this manner, the elements of the entire matrix  $[C]$  can be written as follows:

$$[C] = \begin{bmatrix} C_{11}^{(1)} & & C_{12}^{(1)} & 0 & C_{13}^{(1)} & 0 \\ C_{21}^{(1)} & C_{22}^{(1)} + C_{11}^{(2)} + C_{11}^{(3)} & C_{12}^{(3)} & C_{23}^{(1)} + C_{13}^{(2)} & C_{12}^{(3)} + C_{13}^{(3)} \\ 0 & C_{21}^{(3)} & C_{22}^{(3)} & 0 & C_{23}^{(3)} \\ C_{31}^{(1)} & C_{32}^{(1)} + C_{31}^{(2)} & 0 & C_{33}^{(1)} + C_{33}^{(2)} & C_{32}^{(2)} \\ 0 & C_{21}^{(2)} + C_{31}^{(3)} & C_{32}^{(3)} & C_{23}^{(2)} & C_{22}^{(2)} + C_{33}^{(3)} \end{bmatrix} \quad (11.48)$$

The global matrix has the following properties: (a) It is symmetric, which can be understood if we recall that the local matrices are all symmetric, and (b) it is singular, that is, the determinant formed by its elements is zero, as we shall discuss later.

**4. Equations governing the potentials and solution.** Having obtained the elements of the global matrix, we now set the derivatives of the energy given by (11.45) with respect to the node potentials equal to zero, to minimize the functional, that is, the total energy in the region. Thus,

*Minimization  
of functional*

$$\frac{\partial W}{\partial V_k} = 0, \quad \text{for } k = 1, 2, \dots, n \quad (11.49)$$

For example, from (11.45) and (11.47), we obtain

$$\begin{aligned} \frac{\partial W}{\partial V_1} &= 2C_{11}V_1 + C_{12}V_2 + C_{13}V_3 + C_{14}V_4 \\ &\quad + C_{15}V_5 + C_{21}V_2 + C_{31}V_3 + C_{41}V_4 + C_{51}V_5 \\ &= 0 \end{aligned} \quad (11.50)$$

which gives

$$C_{11}V_1 + C_{12}V_2 + C_{13}V_3 + C_{14}V_4 + C_{15}V_5 = 0 \quad (11.51)$$



In general,

$$\sum_{i=1}^n C_{ki} V_i = 0 \quad \text{for } k = 1, 2, \dots, n \quad (11.52)$$

For the case under consideration,  $n = 5$ , and we get five equations for the five potentials. Noting that the right sides of all five equations are zero, we now observe that the global matrix  $[C]$  must be singular in order to have a nontrivial solution. Since  $[C]$  is singular, it also means that the solution of (11.52) is not unique. The situation is that for a given problem, the potentials are specified at a subset of the global nodes and, hence, we can only use the subset of (11.52) that is pertinent to the derivatives with respect to the unknown potentials. Thus, if the potentials at nodes 1, 3, and 5 are specified, then we use only those two equations resulting from setting  $\partial W/\partial V_2$  and  $\partial W/\partial V_4$  equal to zero to solve for  $V_2$  and  $V_4$ .

Let us now consider an example.

**Example 11.7 Application of finite-element method to an assembly of two triangular elements**

An assembly of two finite elements is shown in Fig. 11.19. Global node 3 is kept at 10-V potential, whereas global node 1 is at 0 V. It is desired to find the values of the potentials at global nodes 2 and 4 by using the finite-element method.

We proceed with the solution by executing the four steps as discussed:

*Step 1:* The region of interest is already discretized. With reference to the numbering of the elements, local nodes, and global nodes, as in Fig. 11.19, we proceed with the remaining three steps as follows.

*Step 2:* Compute the element coefficient matrix for each element. Using (11.45) and (11.44a)–(11.44i) for each of the two elements, we obtain the following values.

**ELEMENT 1**

$$A = 2$$

$$[C^{(1)}] = \begin{bmatrix} 1 & -1/2 & -1/2 \\ -1/2 & 1/2 & 0 \\ -1/2 & 0 & 1/2 \end{bmatrix}$$

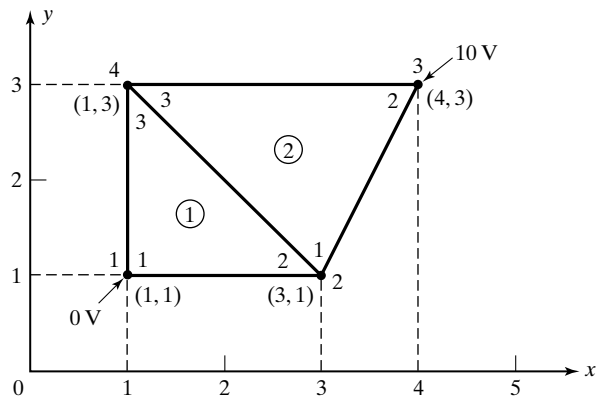


FIGURE 11.19 Assembly of two finite elements for Example 11.7.

**ELEMENT 2**

$$A = 3$$

$$[C^{(2)}] = \begin{bmatrix} 3/4 & -1/2 & -1/4 \\ -1/2 & 2/3 & -1/6 \\ -1/4 & -1/6 & 5/12 \end{bmatrix}$$

Note that for each of  $[C^{(1)}]$  and  $[C^{(2)}]$ , the sum of each row and the sum of each column are zero.

*Step 3:* Compute the global coefficient matrix.

$$[C] = \begin{bmatrix} C_{11}^{(1)} & C_{12}^{(1)} & 0 & C_{13}^{(1)} \\ C_{21}^{(1)} & C_{22}^{(1)} + C_{11}^{(2)} & C_{12}^{(2)} & C_{23}^{(1)} + C_{13}^{(2)} \\ 0 & C_{21}^{(2)} & C_{22}^{(2)} & C_{23}^{(2)} \\ C_{31}^{(1)} & C_{32}^{(1)} + C_{31}^{(2)} & C_{32}^{(2)} & C_{33}^{(1)} + C_{33}^{(2)} \end{bmatrix}$$

$$= \begin{bmatrix} 1 & -1/2 & 0 & -1/2 \\ -1/2 & 5/4 & -1/2 & -1/4 \\ 0 & -1/2 & 2/3 & -1/6 \\ -1/2 & -1/4 & -1/6 & 11/12 \end{bmatrix}$$

*Step 4:* Using

$$\frac{\partial W}{\partial V_2} = 0 \quad \text{and} \quad \frac{\partial W}{\partial V_4} = 0$$

and noting that  $V_1 = 0$  and  $V_3 = 10$  V, we have

$$\begin{bmatrix} -1/2 & 5/4 & -1/2 & -1/4 \\ -1/2 & -1/4 & -1/6 & 11/12 \end{bmatrix} \begin{bmatrix} 0 \\ V_2 \\ 10 \\ V_4 \end{bmatrix} = \begin{bmatrix} 0 \\ 0 \end{bmatrix}$$

or,

$$\begin{aligned} 5V_2 - V_4 &= 20 \\ -3V_2 + 11V_4 &= 20 \end{aligned}$$

Solving, we obtain

$$\begin{aligned} V_2 &= 4.615 \text{ V} \\ V_4 &= 3.077 \text{ V} \end{aligned}$$


---

- K11.6.** Finite-element method; Functional; Minimization of functional; Solution of Laplace’s equation in two dimensions; Element coefficient matrices; Global coefficient matrix.
- D11.7.** For the assembly of four triangular elements in the  $xy$ -plane, shown in Fig. 11.20, find the numerical values of the following elements of the global coefficient matrix: **(a)**  $C_{12}$ ; **(b)**  $C_{25}$ ; **(c)**  $C_{31}$ ; **(d)**  $C_{44}$ ; and **(e)**  $C_{55}$ .
- Ans.* **(a)** 0; **(b)**  $-2$ ; **(c)** 0; **(d)** 2; **(e)** 5.

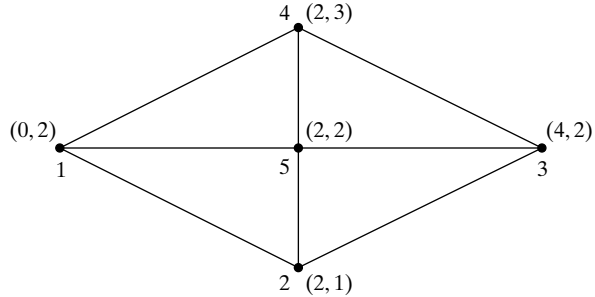


FIGURE 11.20  
For Problem D11.7

### 11.7 FINITE-DIFFERENCE TIME-DOMAIN METHOD

In Section 11.2, we introduced the finite-difference method for solving differential equations. We recall that it consists of replacing the derivatives (with respect to space coordinates) in the differential equations by their finite-difference approximations and solving the resulting algebraic equations. The finite-difference time-domain (FD-TD) method extends this procedure to derivatives involving time variation in addition to the space derivatives, and it is a useful technique for the numerical solution of a wide range of problems in electromagnetics. We shall here include only a very elementary treatment of the topic.

The simplest differential equation involving space and the time variations is the one-dimensional second-order partial differential equation (3.73) given by

$$\frac{\partial^2 E_x(z, t)}{\partial z^2} = \mu_0 \epsilon_0 \frac{\partial^2 E_x(z, t)}{\partial t^2} \tag{11.53}$$

We already know that the solution to this equation consists of a superposition of traveling waves propagating in the  $+z$ -direction and the  $-z$ -direction and, hence, it is known as the *one-dimensional wave equation*. To solve this equation numerically, we discretize the range of interest in  $z$  and replace the left side by its central-difference approximation. Similarly, the time interval of interest can be discretized and the derivative on the right side replaced by its central difference approximation. The resulting algebraic equation can be rearranged to express  $E_x$  at a given point in a space-time ( $z-t$ ) grid of points in

*Solution of one-dimensional wave equation*

terms of its (previously computed) values at certain other neighboring grid points (see Problem P11.29). The rearranged equation thus permits the progressive computation of  $E_x(z, t)$  at the grid points, beginning with its values specified by the boundary conditions and initial conditions pertinent to the problem.

A more illuminating approach, which is also illustrative of the physical phenomenon, emanates from the use of the two first-order coupled partial differential equations (3.72a) and (3.72b), given by

$$\frac{\partial E_x(z, t)}{\partial z} = -\mu_0 \frac{\partial H_y(z, t)}{\partial t} \quad (11.54a)$$

$$\frac{\partial H_y(z, t)}{\partial z} = -\varepsilon_0 \frac{\partial E_x(z, t)}{\partial t} \quad (11.54b)$$

and from which (3.73) was derived. Recall that these equations follow from Maxwell's curl equations for the special case of  $\mathbf{E} = E_x(z, t)\mathbf{a}_x$  and  $\mathbf{H} = H_y(z, t)\mathbf{a}_y$ , and free space for the medium. In the continuous solution of these equations, both  $E_x$  and  $H_y$  are variables defined at the same point  $(z, t)$  in the space-time coordinate system. The starting point in the solution by the FD-TD method is to consider  $E_x$  and  $H_y$  as variables not at the same point, but at alternate points, in the space-time grid, as illustrated, for example, in Fig. 11.21.

Note that the arrangement of Fig. 11.21 leaves certain points in the grid unlabelled and surrounded by four labelled points. For example, the point  $(1, 2)$  is unlabelled and surrounded by the two points  $(0, 2)$  and  $(2, 2)$  labelled  $E_x$  along the line parallel to the  $z$ -axis, and the two points  $(1, 1)$  and  $(1, 3)$  labelled  $H_y$  along the line parallel to the  $t$ -axis. We can use this arrangement to express

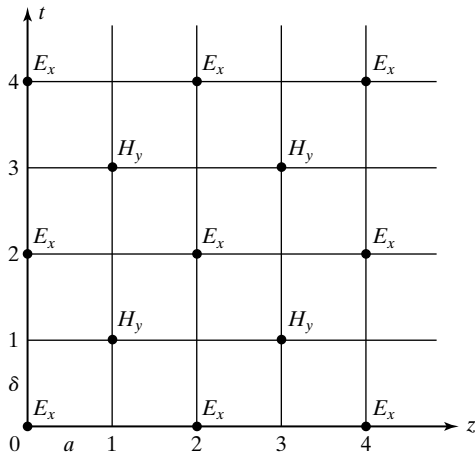


FIGURE 11.21

Space-time grid for the FD-TD solution of the coupled partial differential equations (11.54a) and (11.54b).

$\partial E_x/\partial z$  and  $\partial H_y/\partial t$  at this point in terms of their finite-difference approximations and substitute them in (11.54a). Thus, we have

$$\boxed{\frac{E_x(2, 2) - E_x(0, 2)}{2a} = -\mu_0 \frac{H_y(1, 3) - H_y(1, 1)}{2\delta}} \quad (11.55a)$$

where  $a$  and  $\delta$  are the spacings between the grid points for the  $z$ - and  $t$ -variations, respectively. Similarly, the point  $(2, 3)$  is unlabelled and surrounded by the two points  $(1, 3)$  and  $(3, 3)$  labelled  $H_y$  along the line parallel to the  $z$ -axis, and the two points  $(2, 2)$  and  $(2, 4)$  labelled  $E_x$  along the line parallel to the  $t$ -axis. We can use this arrangement to approximate  $\partial H_y/\partial z$  and  $\partial E_x/\partial t$  at the grid point  $(2, 3)$  to write (11.54b) as

$$\boxed{\frac{H_y(3, 3) - H_y(1, 3)}{2a} = -\varepsilon_0 \frac{E_x(2, 4) - E_x(2, 2)}{2\delta}} \quad (11.55b)$$

Equations (11.55a) and (11.55b) can be used in a “leap-frog” scheme to progress on the grid with the solution. We shall illustrate this by means of an analogous transmission-line example.

---

### Example 11.8 Application of finite-difference time-domain method to an initially charged line

*Initially charged transmission line*

Figure 11.22(a) shows a lossless transmission line of length  $l = 12$  m, characteristic impedance  $Z_0 = 100 \Omega$ , and velocity of propagation  $v_p = 10^8$  m/s, and short-circuited at both ends. At  $t = 0$ , the line current is zero everywhere along the line, and the line voltage has the distribution

$$V(z, 0) = 10 \sin \frac{\pi z}{12} \text{ V}$$

as shown in Fig. 11.22(b). It is desired to apply the FD-TD method to investigate the line voltage and line current for  $t > 0$ .

The differential equations of interest are the transmission-line equations (6.12a) and (6.12b) given by

$$\boxed{\frac{\partial V(z, t)}{\partial z} = -\mathcal{L} \frac{\partial I(z, t)}{\partial t}} \quad (11.56a)$$

$$\boxed{\frac{\partial I(z, t)}{\partial z} = -\mathcal{C} \frac{\partial V(z, t)}{\partial t}} \quad (11.56b)$$

which are analogous to (11.54a) and (11.54b), respectively. From the given values of  $Z_0$  and  $v_p$ , we obtain

$$\mathcal{L} = \frac{Z_0}{v_p} = \frac{100}{10^8} = 10^{-6} \text{ H/m}$$

$$\mathcal{C} = \frac{1}{Z_0 v_p} = \frac{1}{100 \times 10^8} = 10^{-10} \text{ F/m}$$

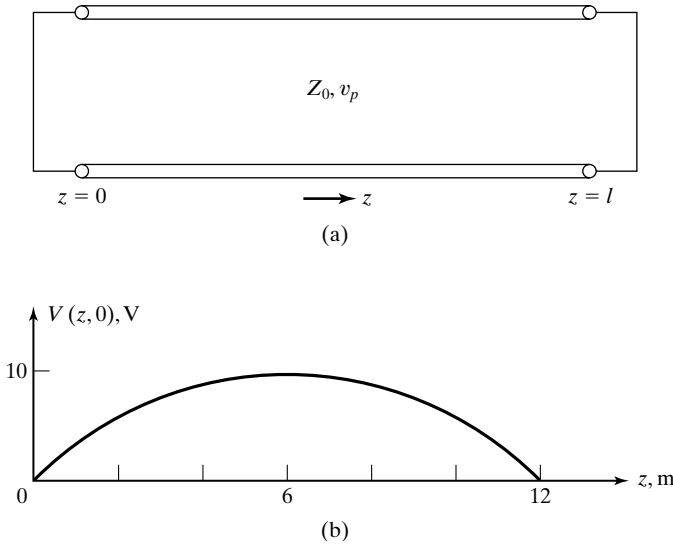


FIGURE 11.22 (a) Lossless transmission line short-circuited at both ends. (b) Voltage distribution on the line for  $t = 0$ .

We shall divide the line into 12 equal segments of width 1 m and use a time step of  $1/v_p = 10^{-8}$  s, so that the space-time grid is as shown in Fig. 11.23. The grid points at which  $V$  is known or to be computed are denoted by circles, and the grid points at which  $I$  is known or to be computed are denoted by crosses. Initial values, as specified by the initial distributions of voltage and current, are marked at the grid points on the  $t = 0$  line. Boundary values of  $V = 0$ , as required by short circuits at either end of the line, are marked at the grid points on the  $z = 0$  ordinate and  $z = 12$  ordinate.

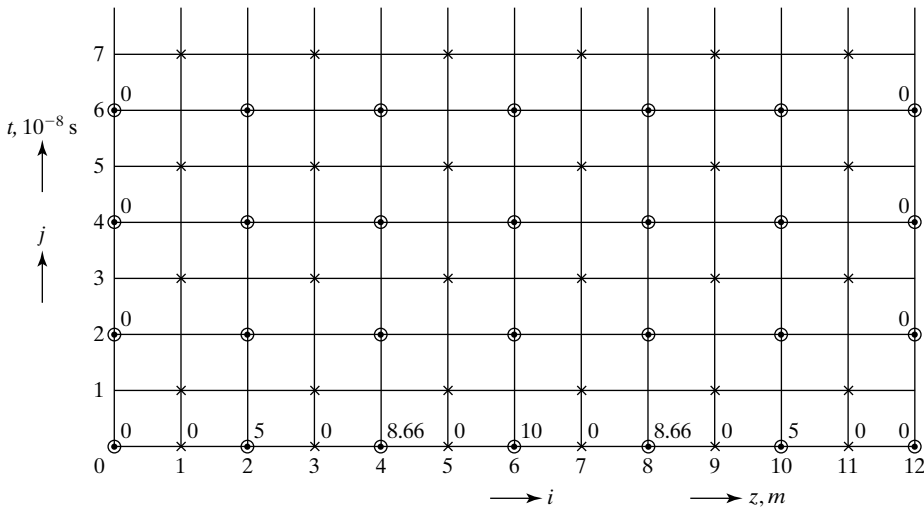


FIGURE 11.23 Space-time grid of points for the FD-TD solution for the line voltage for  $t > 0$  for the transmission line of Fig. 11.22. Numbers beside the circled points represent voltage in volts and those beside the crossed points represent current in amperes.

Denoting the grid points by  $(i, j)$ , where  $i$  refers to space ( $z$ ) and  $j$  refers to time ( $t$ ), and applying the finite-difference approximations to the derivatives in (11.56a), we have

$$\frac{V(i + 1, j - 1) - V(i - 1, j - 1)}{2 \times 1} = -10^{-6} \frac{I(i, j) - I(i, j - 2)}{2 \times 10^{-8}}$$

or

$$I(i, j) = I(i, j - 2) + \frac{V(i - 1, j - 1) - V(i + 1, j - 1)}{100} \tag{11.57}$$

where  $i = 1, 3, 5, 7, 9, 11$ , and  $j = 3, 5, 7, \dots$ . To find the line currents corresponding to  $j = 1$ , we use the initial values of zero corresponding to  $j = 0$  and only one time step. Thus,

$$I(i, 1) = \frac{V(i - 1, 0) - V(i + 1, 0)}{200} \tag{11.58}$$

Applying the finite-difference approximations to the derivatives in (11.56a), we have

$$\frac{I(i + 1, j - 1) - I(i - 1, j - 1)}{2 \times 1} = -10^{-10} \frac{V(i, j) - V(i, j - 2)}{2 \times 10^{-8}}$$

or

$$V(i, j) = V(i, j - 2) + 100[I(i - 1, j - 1) - I(i + 1, j - 1)] \tag{11.59}$$

We can now proceed with the solution, as shown in Table 11.1. To begin the solution, we use (11.58) to compute the values of  $I$  corresponding to  $j = 1$ . Then, we use alternately (11.57) and (11.59) to compute values of  $V$  followed by the values of  $I$  for successive values of  $j$ . The resulting solutions are shown in Table 11.1.

TABLE 11.1 Progression of FD-TD Solution for the Initially Charged Line of Fig. 11.22

	$i \backslash j$	0	1	2	3	4	5	6	7	8	9	10	11	12
V, V	0	0		5		8.66		10		8.66		5		0
I, A	0		0		0		0		0		0		0	
I, A	1		-0.025		-0.0183		-0.0067		0.0067		0.0183		0.025	
V, V	2	0		4.33		7.50		8.66		7.50		4.33		0
I, A	3		-0.0683		-0.05		-0.0183		0.0183		0.05		0.0683	
V, V	4	0		2.50		4.33		5.00		4.33		2.50		0

The values of  $i$  and  $j$  correspond to the space-time grid in Fig. 11.23.

The continuous solution to this problem can be obtained by using the procedures discussed in Section 6.5 for time-domain analysis of transmission lines with initial conditions, or by using the natural oscillations concepts in Section 7.1. This solution is given exactly by

*Magic time step*

$$V(z, t) = 10 \sin \frac{\pi z}{12} \cos \frac{10^8 \pi t}{12} \text{ V}$$

It can be seen that the computed values of  $V$  at the grid points agree with the exact analytical solution. In fact, it can be shown that this is the case when the grid points are chosen such that the time increment is equal to the so-called “magic time step,”<sup>1</sup> which is the space segment width divided by the velocity of propagation. The solution may, however, be insufficient to represent the actual behavior in the continuous region if the discretization in  $z$  does not correspond to a fraction of a wavelength. A discussion of such considerations as accuracy of the solution and stability of the solution process is beyond the scope here.

**K11.7.** Finite-difference time-domain method; One-dimensional second-order partial differential equation; First-order coupled partial differential equations; Leap-frog scheme.

**D11.8.** For the transmission-line problem of Example 11.8, extend the solution beyond the grid points in Table 11.1 to find the following quantities: **(a)**  $I(5, 3)$ ; **(b)**  $V(6, 8)$ ; **(c)**  $I(7, 7)$ ; and **(d)**  $V(8, 4)$ .

*Ans.* **(a)**  $-0.0683 \text{ A}$ ; **(b)**  $0 \text{ V}$ ; **(c)**  $0.025 \text{ A}$ ; **(d)**  $-4.33 \text{ V}$ .

## SUMMARY

In this chapter, we considered several solution techniques, including the analytical technique of *separation of variables*, the geometrical method of *field mapping*, and four numerical methods: (1) the finite-difference method, (2) the method of moments, (3) the finite-element method, and (4) the finite-difference time-domain method.

We illustrated the solution of the Laplace’s equation in two dimensions

$$\frac{\partial^2 V}{\partial x^2} + \frac{\partial^2 V}{\partial y^2} = 0 \quad (11.60)$$

by using the *separation of variables* technique, and considered two examples involving the determination of the potential distribution inside a rectangular slot cut in a semi-infinite plane conducting slab held at zero potential and for a specified potential distribution at the mouth of the slot. For the *field mapping* technique, we illustrated it by considering a transmission line with arbitrary cross section and finding the line parameters.

<sup>1</sup>See A. Taflove, *Computational Electrodynamics; The Finite-Difference Time-Domain Method* (Norwood, MA: Artech House, 1995), p. 38.



The finite-difference method is based on replacing the derivative terms in a differential equation by their finite-difference approximations and solving the resulting algebraic equations. We illustrated the technique by applying it to a one-dimensional differential equation. We then discussed and illustrated by means of an example the numerical solution of (11.60). The numerical solution is based on the finite-difference approximation to (11.60), where the potential  $V_0$  at a point  $P$  in the charge-free region is given by

$$V_0 \approx \frac{1}{4}(V_1 + V_2 + V_3 + V_4) \quad (11.61)$$

where  $V_1, V_2, V_3,$  and  $V_4$  are the potentials at four equidistant points lying along mutually perpendicular axes through  $P$ . By using an iterative technique, a set of values for the potentials at appropriately chosen grid points is obtained such that the potential at each grid point satisfies (11.61) to within a specified tolerance.

We then turned our attention to the method of moments, which is a numerical technique useful for solving a class of problems for which exact analytical solutions are in general not possible. Considering, for example, a surface charge distribution  $\rho_S(x, y, z)$  on a given surface, the method of moments technique consists of inverting the integral equation

$$V(x, y, z) = \frac{1}{4\pi\epsilon_0} \int_{\substack{\text{surface of} \\ \text{the charge} \\ \text{distribution}}} \frac{\rho_S(x', y', z')}{R} dS'$$

by approximating the integral as a summation. We illustrated the method of moments technique by means of two examples: (1) finding the charge distribution on a thin, straight wire held at a known potential and (2) finding the capacitance of a parallel-plate capacitor, taking into account fringing of the field at the edges of the plates.

We then applied the method of moments and the finite-difference method to the determination of transmission-line parameters. Specifically, we illustrated the determination of  $Z_0$  and  $v_p$  for a parallel-strip line embedded in a homogeneous medium by using the method of moments and for an enclosed-microstrip line by using the finite-difference method.

The finite-element method, a more general technique than the finite-difference method for solving differential equations, is based on the minimization of an integral-type functional such as the electric energy in the case of the electric potential, instead of solving the differential equations directly. The solution procedure consists of (1) discretizing the region of interest into a set of finite elements, (2) deriving the governing equations for the individual finite elements, (3) relating the individual elements to the assembly of the elements, and (4) obtaining and solving the system of equations for the potentials.

We illustrated this procedure for the solution of the two-dimensional Laplace's equation (11.60) by considering triangles for the finite elements. A linear variation is assumed for the potential within each triangle and the *element*

*coefficient matrix* that relates the energy within the triangle to the potentials at the vertices of the triangle is derived. A *global coefficient matrix* that relates the assembly of elements to the individual element is then obtained and used to complete the solution. We considered an example involving an assembly of two triangles with the potentials specified at two of the four global nodes and computed the two unknown potentials to illustrate this procedure.

The finite-difference time-domain method extends the numerical technique to solving differential equations involving time. A simple example is the solution of the one-dimensional wave equation, consisting of replacing the second derivatives with respect to the spatial dimension and time by the corresponding central-difference approximations and applying the resulting algebraic equation to a space-time grid of points. Alternatively, two first-order coupled partial differential equations following from Maxwell's curl equations can be used in a more illuminating manner by applying their approximations to a space-time grid of points in a "leap-frog" scheme. We illustrated this procedure by considering a lossless transmission line initially charged to a voltage, and finding the line voltage and current values at points on the line at a later value of time.

## REVIEW QUESTIONS

- Q11.1.** Outline the solution of Laplace's equation in two dimensions by the separation of variables technique.
- Q11.2.** Describe the formulation behind the finite-difference method of solving differential equations.
- Q11.3.** Outline the procedure for solving a one-dimensional differential equation by the finite-difference method.
- Q11.4.** Discuss the basis behind the numerical solution of Laplace's equation in two dimensions by the finite-difference method.
- Q11.5.** Describe the iteration technique for the computer solution of Laplace's equation in two dimensions by the finite-difference method.
- Q11.6.** How would you apply the iteration technique for the computer solution of Laplace's equation in three dimensions?
- Q11.7.** Discuss the formulation behind the problem of finding the charge distribution on a conductor of known potential by the method of moments.
- Q11.8.** Outline by means of an example the procedure for obtaining the charge distribution on a conductor of known potential by the method of moments technique.
- Q11.9.** Why is the expression for the capacitance of a parallel-plate capacitor obtained by using Laplace's equation in one dimension approximate?
- Q11.10.** Discuss the determination of the capacitance of a parallel-plate capacitor by the method of moments technique.
- Q11.11.** Describe the procedure for obtaining  $Z_0$  and  $v_p$  for a parallel-strip line embedded in a homogeneous medium by using the method of moments.
- Q11.12.** Outline the procedure for obtaining  $Z_0$  and  $v_p$  for an enclosed-microstrip line by using the finite-difference method.

- Q11.13.** Describe the procedure for computing the transmission-line parameters by using the field mapping technique.
- Q11.14.** Describe the basic concept of the finite-element method for solving differential equations and outline the steps involved in its implementation.
- Q11.15.** Discuss the linear approximation for the potential within a triangular finite element.
- Q11.16.** Discuss the functional to be minimized for the solution of Laplace's equation in two dimensions by the finite-element method.
- Q11.17.** Discuss the derivation of the element coefficient matrix for a triangular finite element, and describe its properties.
- Q11.18.** Describe the determination of the global coefficient matrix for an assembly of triangular elements from the individual element coefficient matrices and discuss its properties.
- Q11.19.** Describe the solution of the one-dimensional wave equation by the FD-TD method.
- Q11.20.** Discuss the key to the solution of Maxwell's curl equations for the special case of  $\mathbf{E} = E_x(z, t)\mathbf{a}_x$  and  $\mathbf{H} = H_y(z, t)\mathbf{a}_y$ , and free space for the medium, by the FD-TD method, as compared to the solution of the one-dimensional wave equation.
- Q11.21.** Describe the "leap-frog" scheme of carrying out the FD-TD solution to the transmission-line equations for the lossless case.
- Q11.22.** Discuss the agreement between the values of  $V$  computed by the FD-TD method in Example 11.8 with those provided by the exact analytical solution.

## PROBLEMS

### Section 11.1.

- P11.1. Application of analytical solution of Laplace's equation in two dimensions.** The potential distribution at the mouth of the slot of Fig. 11.1 is given by

$$V = V_0 \sin \frac{\pi y}{b} + \frac{1}{3} V_0 \sin \frac{3\pi y}{b}$$

(a) Find the solution for the potential distribution inside the slot. (b) Compute the value of the potential at the center of the slot, assuming the slot to be square.

- P11.2. Application of analytical solution of Laplace's equation in two dimensions.** Repeat Problem 11.1 for the potential distribution at the mouth of the slot given by

$$V = V_0 \sin^3 \frac{\pi y}{b}$$

- P11.3. Application of analytical solution of Laplace's equation in two dimensions.** Assume that the rectangular slot of Fig. 11.1 is covered at the mouth by conducting plates such that the potential distribution is given by

$$V = \begin{cases} 0 & \text{for } 0 < y < b/4 \\ V_0 & \text{for } b/4 < y < 3b/4 \\ 0 & \text{for } 3b/4 < y < b \end{cases}$$

Find the solution for the potential inside the slot.

**P11.4. Using the solution of Laplace's equation for the potential to find the electric field.**

For the rectangular slot of Example 11.1, (a) find the expression for the electric field intensity inside the slot and (b) find the electric field intensity at the center of the slot, assuming the slot to be square.

**Section 11.2****P11.5. Solution of a one-dimensional differential equation by finite-difference method.**

By discretizing the region between  $x = 0$  and  $x = 1$  into five equal segments spaced 0.2 apart and applying the finite-difference method, solve for the approximate values of  $f$  at the four interior grid points for the one-dimensional differential equation

$$\frac{d^2f(x)}{dx^2} + 4f(x) = 0$$

with the boundary conditions specified as  $f(0) = 0$  and  $f(1) = 1$ . Compare your answers with the exact solution to the differential equation.

**P11.6. Finite-difference method of solution of Laplace's equation in two dimensions.**

The cross section of an infinitely long arrangement of conductors normal to the page and that repeats endlessly in the plane of the page is shown in Fig. 11.24. For the grid points shown, find the values of  $V_1, V_2, V_3, V_4,$  and  $V_5$ , by writing equations consistent with (11.20) and solving them. Then find the approximate magnitude of the field intensity at grid point 2 and the approximate value of the surface charge density at point  $P$ , assuming that the spacing between the grid points is  $d$  and the medium between the conductors is free space.

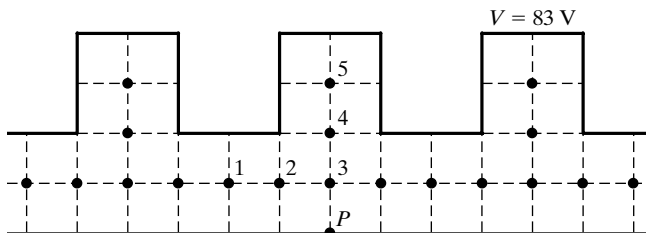


FIGURE 11.24

For Problem P11.6.

**P11.7. Finite-difference method of solution of Laplace's equation in two dimensions.**

The cross section of an arrangement of conductors, infinitely long and normal to the page, is square, as shown in Fig. 11.25. Three sides are kept at 0 V and the fourth side is kept at 28 V. The region between the conductors is divided into a  $4 \times 4$  grid of squares. Although there are nine grid points, there are only six unknown potentials  $V_A, V_B, \dots, V_F$ , because of symmetry. (a) By writing equations consistent with (11.20) for these six potentials and solving the equations, find the values of the potentials. (b) Find the approximate magnitude of the electric field intensity at grid point  $B$ , assuming that the spacing between grid points is  $d$ . (c) Find the approximate surface charges per unit length of the arrangement on the 28-V conductor and the 0-V conductor.

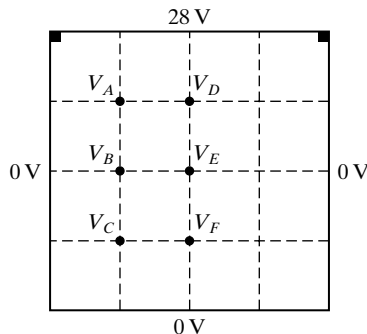


FIGURE 11.25  
For Problem P11.7.

**P11.8. Modification of solution by finite-difference method for an inhomogeneous medium.** In Fig. 11.4, assume that the region below the  $y$ -axis ( $x < 0$ ) is a perfect dielectric of relative permittivity  $\epsilon_r$ , whereas the region above the  $y$ -axis ( $x > 0$ ) is free space. Show that the modified form of (11.20) is then given by

$$V_0 \approx \frac{V_1 + \epsilon_r V_2}{2(1 + \epsilon_r)} + \frac{V_3 + V_4}{4}$$

**P11.9. Modification of solution by finite-difference method for unequal grid spacing.** For unequal spacings between grid points, as shown in Fig. 11.26, show that the generalization of (11.20) is given by

$$V_0 = \frac{V_1}{(1 + d_1/d_2)(1 + d_1 d_2/d_3 d_4)} + \frac{V_2}{(1 + d_2/d_1)(1 + d_2 d_1/d_4 d_3)} + \frac{V_3}{(1 + d_3/d_4)(1 + d_3 d_4/d_2 d_1)} + \frac{V_4}{(1 + d_4/d_3)(1 + d_4 d_3/d_1 d_2)}$$

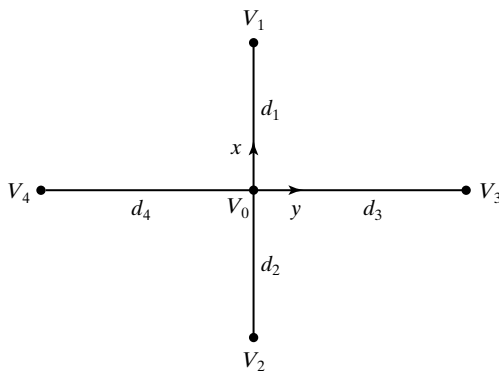


FIGURE 11.26  
For Problem P11.9.

### Section 11.3

**P11.10. Application of method of moments to a bent wire held at a known potential.** Consider a thin, straight cylindrical wire of length  $l$  and radius  $a$  ( $\ll l$ ) bent in the middle to make a  $90^\circ$  angle and held at a potential of 1 V. By dividing the

wire into four equal segments and assuming the charge density in each segment to be uniform, and using the method of moments, find the total charge on the wire if  $l = 1 \text{ m}$  and  $a = 1 \text{ mm}$ . To compute the potential at the center of a given segment due to the charge in another segment, assume the charge to be a point charge at the center of that segment.

- P11.11. Application of method of moments to a square-shaped wire held at a known potential.** Consider a thin wire of radius  $1 \text{ mm}$  bent into the form of a square of sides  $60 \text{ cm}$  and held at a potential of  $1 \text{ V}$ . By dividing each side of the square into three equal segments and assuming the charge density in each segment to be uniform, and using the method of moments, find the total charge on the wire. To compute the potential at the center of a given segment due to the charge in another segment, assume the charge to be a point charge at the center of that segment.
- P11.12. Capacitance of an arrangement of two square-shaped wires by method of moments.** Consider two thin wires that are square-shaped as in Problem P11.11 and arranged such that the sides of one wire are directly above and parallel to the sides of the second wire at a spacing of  $10 \text{ cm}$ , so as to form a capacitor. Using the method of moments as in Problem P11.11, find the capacitance of the arrangement.
- P11.13. Application of method of moments to a square-shaped conductor with a square hole.** A square-shaped conductor of area  $3a \times 3a$ , with a square-shaped hole of area  $a \times a$  in the middle, as shown in Fig. 11.27, is held at a potential of  $1 \text{ V}$ . By dividing the conductor into eight squares, as shown in the figure, and using the method of moments, find the total charge on the conductor. To find the potential at the center point of a square due to the charge in another square, consider the charge in that square to be a point charge at the center of that square.

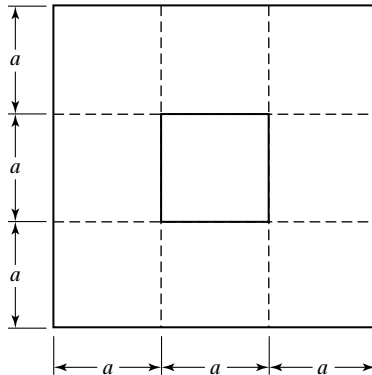


FIGURE 11.27

For Problem P11.13.

- P11.14. Capacitance of an arrangement of two square-shaped conductors with square holes.** Assume that a capacitor is made up of two parallel conductors, each having the shape shown in Fig. 11.27. If the spacing between the plates is  $a$ , find the capacitance of the arrangement by dividing each conductor into squares, as shown in Fig. 11.27, and applying the method of moments.
- P11.15. Capacitance for a square-shaped conductor above a square-holed conductor.** The arrangement shown in Fig. 11.28 is that of a capacitor obtained by removing

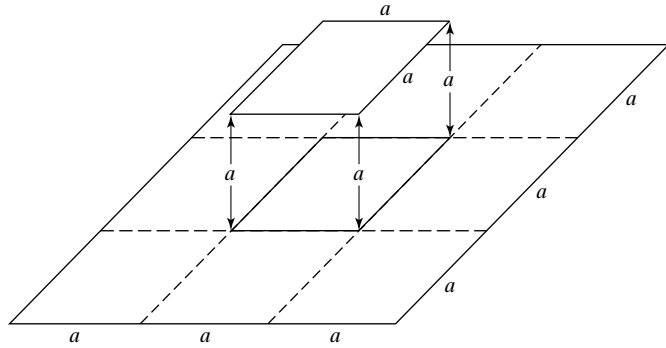


FIGURE 11.28  
For Problem P11.15.

a square-shaped part of sides  $a$  from the center of a square-shaped conductor of sides  $3a$  and displacing it by distance  $a$  directly above the hole. By dividing the lower plate as shown in the figure, find the capacitance of the arrangement.

- P11.16. Application of method of moments to a cube-shaped conductor.** A conductor having the shape of a cube of sides  $a$  is held at a potential of 1 V. By dividing each side into a  $2 \times 2$  set of squares, assuming the charge density in each square to be uniform, and using the method of moments, find the total surface charge on the conductor. To find the potential at the center of a square due to the charge in another square, consider the charge in that square to be a point charge at the center of the square.

**Section 11.4**

- P11.17. Determination of parallel-strip line parameters by using method of moments.** For the parallel-strip line of Example 11.5, repeat the solution by considering the charges to be line charges along the centerlines of the substrips for writing the contributions to the potential difference between a given pair of substrips due to the charges in a different pair of substrips and using the formula given in Problem P5.12.
- P11.18. Application of method of moments to a parallel-strip line of unequal conductor widths.** Consider a parallel-strip line with unequal widths of the conductors, as shown in Fig. 11.29. Obtain the characteristic impedance of the line for the case of  $k = 1$  by dividing the conductors into substrips as shown in the figure and using the method of moments. Note that from considerations of symmetry, there are only three unknown charge densities  $\rho_{S1}$ ,  $\rho_{S2}$ , and  $\rho_{S3}$ . Write two equations

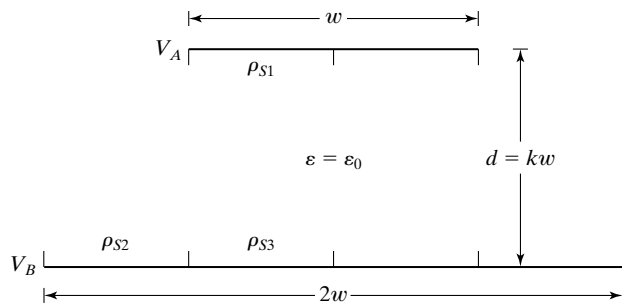


FIGURE 11.29  
For Problem P11.18.

by equating the expressions for the potential differences  $V_{12}$  and  $V_{13}$  to  $(V_A - V_B)$  and the third equation from consideration of charge neutrality. Use the result of Problem P5.12 for writing the contributions to the potential differences in all cases.

**P11.19. Application of method of moments to coaxial conductors of square cross sections.**

Consider a transmission line having the cross-sectional view shown in Fig. 11.30. With the conductors of the line divided into substrips as shown in the figure, obtain the characteristic impedance by using the method of moments. Note that from considerations of symmetry, there are only three unknown charge densities  $\rho_{s1}$ ,  $\rho_{s2}$ , and  $\rho_{s3}$ . Write two equations by equating the expressions for the potential differences  $V_{12}$  and  $V_{13}$  to  $(V_A - V_B)$  and the third equation from consideration of charge neutrality. For writing the contribution to the potential difference between a given pair of substrips due to one of those substrips, use the result of Problem P5.12. But for writing the contribution to the potential difference between a given pair of substrips due to a third substrip, consider the charge in that substrip to be a line charge along the centerline of the substrip.

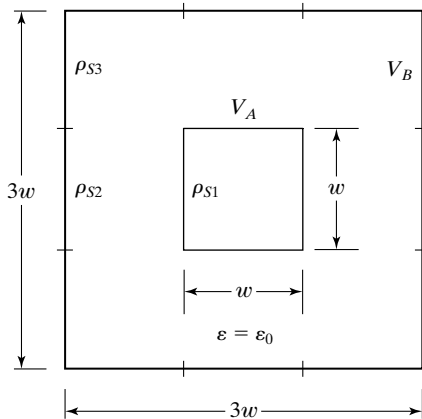


FIGURE 11.30

For Problem P11.19.

**P11.20. Determination of enclosed-microstrip line parameters by finite-difference method.**

For the enclosed-microstrip line of Fig. 11.13, repeat the computations of  $\mathcal{C}$ ,  $\mathcal{C}_0$ ,  $Z_0$ , and  $v_p$ , by finding the magnitude of the charge per unit length by considering the contour that passes through the center points of the squares adjacent to the center conductor, instead of the one shown in the figure.

**Section 11.5.**

**P11.21. Application of field mapping by the curvilinear squares technique to a coaxial cable.**

By applying the curvilinear squares technique to a coaxial cable of inner radius  $a$  and outer radius  $b$ , show that the characteristic impedance of the cable is  $(\eta/2\pi) \ln b/a$ , where  $\eta$  is the intrinsic impedance of the dielectric of the cable.

**P11.22. Field mapping by the curvilinear squares technique for an eccentric coaxial cable.**

The cross section of an eccentric coaxial cable [see Fig. 5.13(d)] consists of an outer circle of radius  $a = 5$  cm and an inner circle of radius  $b = 2$  cm, with their centers separated by  $d = 2$  cm. By constructing a field map consisting of curvilinear squares, obtain the approximate value of  $Z_0$  in terms of  $\eta$  of the dielectric.



**P11.23. Field mapping by the curvilinear squares technique for a shielded-strip line.**

When one microstrip line is inverted and placed on top of another microstrip line, as shown by the cross-sectional view in Fig. 11.31, a shielded strip line is obtained. Although the sandwich arrangement of this line is more difficult to fabricate than is the microstrip line, it has the advantage that the fields are confined mostly to the substrate region. Assuming for simplicity that the fields are confined to the substrate region, construct a field map consisting of curvilinear squares and compute the approximate value of  $Z_0$  of the line, for the dimensions shown in Fig. 11.31, and considering the substrate to be a perfect dielectric having  $\epsilon = 9\epsilon_0$  and  $\mu = \mu_0$ .

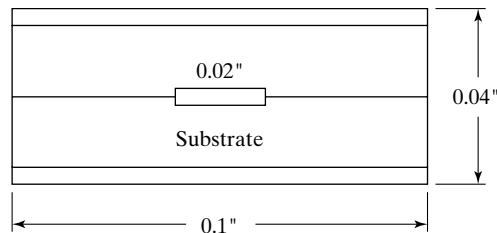


FIGURE 11.31  
For Problem P11.23.

**P11.24. Method of curvilinear squares for a line with cross section of circle inside a square.**

Consider a transmission line having the cross section shown in Fig. 11.32. The inner conductor is a circle of radius  $a$  and the outer conductor is a square of sides  $2a$ . Find the approximate value of the characteristic impedance of the line, by using the method of curvilinear squares.

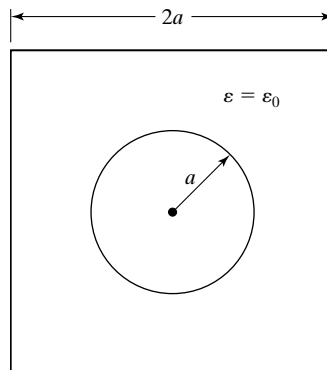


FIGURE 11.32  
For Problem P11.24.

**Section 11.6****P11.25. Alternate representation for the element coefficient matrix in finite-element method.** Alternative to the representations (11.44a)–(11.44i), show that the elements of the element coefficient matrix  $[C^{(e)}]$  in (11.43c) can be written as

$$[C^{(e)}] = \frac{1}{2} \begin{bmatrix} \cot \theta_2 + \cot \theta_3 & -\cot \theta_3 & -\cot \theta_2 \\ -\cot \theta_3 & \cot \theta_1 + \cot \theta_3 & -\cot \theta_1 \\ -\cot \theta_2 & -\cot \theta_1 & \cot \theta_1 + \cot \theta_2 \end{bmatrix}$$

where  $\theta_1, \theta_2,$  and  $\theta_3$  are the interior angles at the vertices 1, 2, and 3, respectively, of the triangular element, as shown in Fig. 11.33.

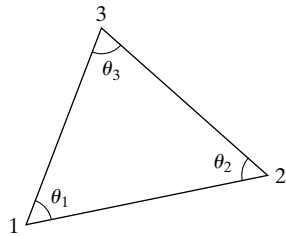


FIGURE 11.33  
For Problem P11.25.

**P11.26. Application of the finite-element method to an assembly of two triangular elements.** Solve Example 11.7 by discretizing the region Fig. 11.19, as shown in Fig. 11.34.

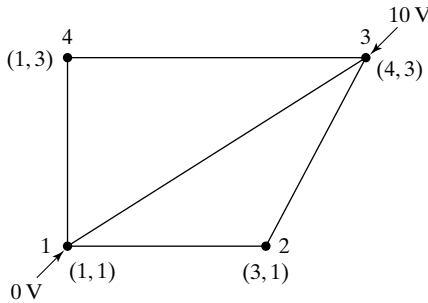


FIGURE 11.34  
For Problem P11.26.

**P11.27. Application of the finite-element method to an assembly of three triangular elements.** By discretizing the region of Fig. 11.19 into three triangles, as shown in Fig. 11.35, solve for the potentials at global nodes 2, 4, and 5.

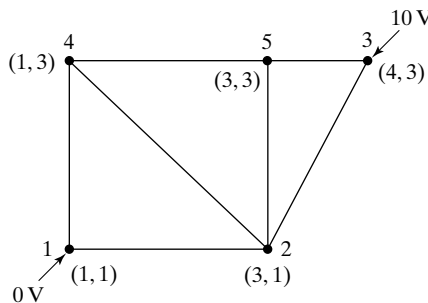


FIGURE 11.35  
For Problem P11.27.

**P11.28. Application of the finite-element method to an assembly of three triangular elements.** Repeat Problem P11.27 for the region of Fig. 11.19 discretized into three triangles, as shown in Fig. 11.36.

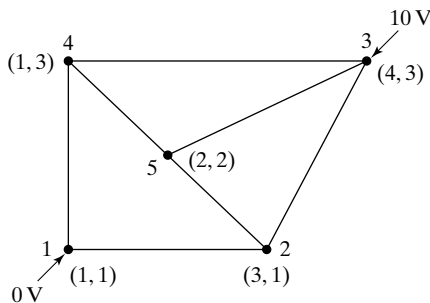


FIGURE 11.36  
For Problem P11.28.

### Section 11.7

**P11.29. Application of central-difference approximation to derivatives in wave equation.** Show that the application of the central-difference approximation to the derivatives in (11.53) in conjunction with the space-time grid of Fig. 11.21 gives the result

$$E_x(i, j + 1) = \left( 2 - 2 \frac{\delta^2 c^2}{a^2} \right) E_x(i, j) + \frac{\delta^2 c^2}{a^2} [E_x(i + 1, j) + E_x(i - 1, j)] - E_x(i, j - 1)$$

where  $i$  and  $j$  refer to space ( $z$ ) and time ( $t$ ), respectively, and  $c = 1/\sqrt{\mu_0 \epsilon_0}$ .

**P11.30. Application of finite-difference time-domain method to an initially charged line.** In Example 11.8, assume that

$$V(z, 0) = 10 \sin \frac{\pi z}{6} \text{ V}$$

Using the same space-time grid as in Fig. 11.23, prepare a table similar to Table 11.1 for obtaining values of  $V$  at the grid points corresponding to  $j = 4$ .

**P11.31. Application of finite-difference time-domain method to an initially charged line.** Repeat Problem 11.30 for

$$V(z, 0) = 10 \sin^3 \frac{\pi z}{12} \text{ V}$$

**P11.32. Application of finite-difference time-domain method to an initially charged line.** Repeat Problem 11.30 for

$$V(z, 0) = \begin{cases} \frac{5}{3}z & \text{for } 0 \leq z \leq 6 \\ 20 - \frac{5}{3}z & \text{for } 6 \leq z \leq 12 \end{cases}$$

### REVIEW PROBLEMS

**R11.1. Application of analytical solution of Laplace's equation in two dimensions.** Assume that the rectangular slot of Fig. 11.1 is covered at the mouth by conducting

plates such that the potential distribution is given by

$$V = \begin{cases} V_0 & \text{for } 0 < y < b/2 \\ -V_0 & \text{for } b/2 < y < b \end{cases}$$

Find the solution for the potential inside the slot.

- R11.2. Capacitance of rectangular-shaped conductors at right angles by method of moments.** Consider two thin rectangular-shaped conductors of size  $a \times 3a$  arranged as shown in Fig. 11.37. By dividing each conductor into three squares of sides  $a$  and applying the method of moments, find the capacitance of the arrangement. To find the potential at the center of a square due to the charge on another square, consider the charge on that square to be a point charge at the center of that square.

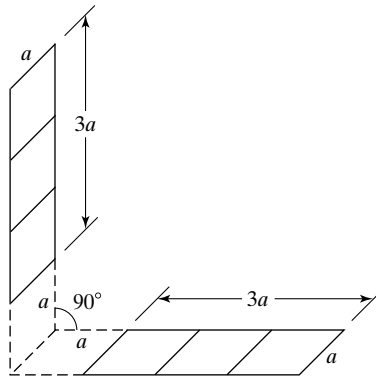


FIGURE 11.37

For Problem R11.2.

- R11.3. Finite-difference method for a line with cross section of circle inside a square.** Consider a transmission line having the cross section shown in Fig. 11.38. The inner conductor is a circle of radius  $a$  and the outer conductor is a square of sides  $2a$ . Using the grid points as shown in the figure and applying the finite-difference method, find the approximate value of the characteristic impedance of the line. (*Hint:* Use the result of Problem P11.9 for grid point 6.)

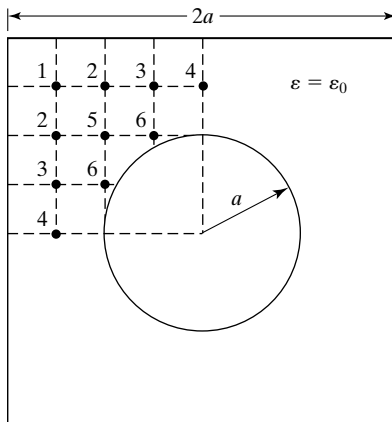


FIGURE 11.38

For Problem R11.3.

**R11.4. Consistency of finite-element method with finite-difference method.** Consider a square region divided into four right isosceles triangular finite elements, as shown in Fig. 11.39. Show that for linear variation of potential within each element, as represented by (11.31), the electric energy is proportional to the sum of the squares of the differences between the potential at global node 5 (the 90°-vertex) and the remaining two nodes (the 45°-vertices). For example, for element 1, it is proportional to  $[(V_1 - V_5)^2 + (V_2 - V_5)^2]$ . Further show that the finite-element method gives the same result for  $V_5$  in terms of  $V_1, V_2, V_3,$  and  $V_4$ , as that given by the finite-difference method, that is,

$$V_5 = \frac{1}{4}(V_1 + V_2 + V_3 + V_4)$$

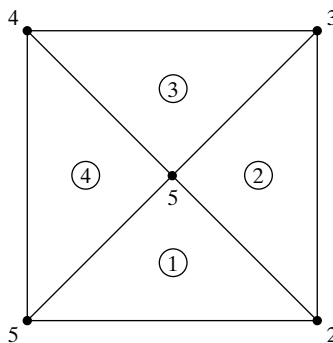


FIGURE 11.39  
For Problem R11.4.

**R11.5. Application of finite-difference time-domain method to an initially charged line.** Repeat the solution of Example 11.8 up to  $t = 4 \times 10^{-8}$  s for each of the following two cases: **(a)** time step =  $2 \times 10^{-8}$  s and **(b)** time step =  $0.5 \times 10^{-8}$  s. For each case, compare the values of  $V$  obtained for  $t = 4 \times 10^{-8}$  s with those from the exact analytical solution and comment on your results.